Rigidity Theory of Graphs with Heterogeneous Vertices

Yongjie Liu[1], Gangshan Jing[2*], and Long Wang[1*]

[1] Center for Systems and Control, College of Engineering, Peking University, Beijing 100871, China

[2] School of Automation, Chongqing University, Chongqing 400044, China

[*] Corresponding authors. E-mail: jinggangshan@cqu.edu.cn, longwang@pku.edu.cn

Abstract

Graph rigidity theory answers the question of whether a set of local constraints can uniquely determine the shape of a graph embedded in a Euclidean space, and has been recognized as a useful tool of examining solvability of sensor network localization (SNL) problems. In recent years, constraints involving signed angle (SA) and ratio of distance (RoD) have been adopted in SNL due to their ease of measurements and independence of the global coordinate. However, most prior works consider homogeneous nodes, i.e., all the sensors have the same perceptual abilities. Although mixed constraints have been considered recently, little is known about how the bipartition of nodes based on perceptual abilities affects the rigidity property of the network.

In this paper, we propose a novel SA-RoD rigidity theory for graphs with heterogeneous vertices, where each vertex corresponds to a sensor node capturing either SA or RoD measurements. Unlike existing rigidity theory, the SA-RoD rigidity is shown to be strongly dependent on bipartitions of nodes, and exhibits a duality. Moreover, the shape of an SA-RoD constrained network can be uniquely determined up to uniform rotations, translations, and scalings (global SA-RoD rigidity) even if it is neither globally RoD rigid nor globally SA rigid. A scalable approach to construction of globally SA-RoD rigid frameworks is proposed. Localizability analysis and localization algorithm synthesis are both conducted based on weaker network topology conditions, compared with SA- or RoD-based SNL. Numerical simulations are worked out to validate the theoretical results.

1 Introduction

Multiagent systems have been extensively investigated in various cooperative settings, such as consensus [1, 2, 3, 4], flocking [5, 6], swarm control [7], formation control [8, 9], network localization [10], and distributed optimization [11]. It is well-known that cooperative behaviors are fundamentally shaped by the topology of interaction networks. To model the interaction topology, graph theory is commonly employed as a powerful tool. As an important branch of graph theory, graph rigidity theory investigates whether the shape of a framework can be uniquely determined by certain geometrical constraints. In the presence of diverse geometric constraints, traditional distance rigidity theory has been extended to bearing rigidity [12], angle rigidity [13], signed angle (SA) rigidity [14][15], and ratio-of-distance (RoD) rigidity [16]. Furthermore, these theories have been extensively applied to sensor network localization (SNL), which aims to localize a network when the positions of some nodes (anchors) and relative measurements are provided. According to the sensing capabilities of sensors, SNL can be roughly classified depending on the type of measurements: relative position[17, 18], distance [19, 20], bearing [21, 22], angle [23], signed angle [24].

To deal with more general constraints in practice, various rigidity theories mixing different types of constraints have been developed in recent years. [25] mixes constraints of distances and bearings, and establishes a combinatorial characterization of rigidity. [26] mixes constraints of bearings and RoDs to propose a bearing-ratio-of-distance (B-RoD) rigidity theory, and shows the equivalence among (infinitesimal/global) B-RoD rigidity and graph connectivity. [27] mainly mixes distances (or angles) and signed normalized areas (or volumes) to address the flip and flex ambiguity. In [28, 29], the authors mix angles and displacements to study the shape uniqueness problem. [30] performs an abstract analysis on the role of symmetry induced by general Lie-group actions in rigidity for heterogeneous and non-Euclidean state spaces. In summary, geometric constraints (distance, bearing, angle, SA, RoD, displacement) in most existing works are defined through edges, with little consideration given to node-based attributes. However, different types of edge constraints often stem from different attributes of nodes, a situation frequently seen in reality.

Building on aforementioned developments, rigidity theories based on mixing different types of measurement have been utilized in SNL problems to examine network localizability [31, 21, 24]. In [32], the author provides graphical criteria for localizability and design SNL algorithms under hybrid distance-bearing information. In [33, 28, 29], the authors study SNL by constructing linear displacement constraints for locations of nodes using mixed types of local relative measurements. Despite these interesting works on SNL with mixed measurements, the advantages of heterogeneous nodes have yet to be explored. More specifically, how to assign the sensing capabilities to the nodes to ensure network localizability has rarely been discussed.

In this paper, we consider SNL with heterogeneous sensors, where each node can only sense one type of measurements (SA or RoD). Accordingly, an SA-RoD rigidity theory based on heterogeneous nodes is developed. The reason of mixing SA and RoD constraints lies in the following three aspects. 1) There exist similar algebraic properties between SA and RoD. That is, two SAs (or RoDs) sharing a common edge can be algebraically combined through addition or subtraction (multiplication or division) to derive a third SA (or RoD). Furthermore, for any polygon in $\mathbb{R}^2$, the sum of all SAs under a consistent orientation is congruent to 0 modulo π. Similarly, the ordered product of all RoDs must equal 1. 2) SA and RoD constraints share the same trivial infinitesimal motions, namely, uniform rotations, translations, and scalings. 3) SAs and RoDs are practically measurable by a Bluetooth 5.1 module [34] and a monocular camera [16], respectively. Moreover, both measurements are independent of the global coordinate. Since only one type of measurements can be accessed by each node, the geometric constraints of a sensor network are naturally linked to the bipartition of heterogeneous nodes. The bipartition plays a key role in the rigidity of the underlying framework. Compared with traditional rigidity theory, the number of edges required to guarantee the rigidity property of frameworks can be further reduced. This is the most distinctive feature of our developed theory.

The main contributions of this work can be summarized as follows.

1) The SA-RoD rigidity theory in $\mathbb{R}^2$ is established. It is shown that the shape of a framework can be uniquely determined by SA-RoD constraints up to uniform rotations, translations, and scalings if it is globally SA-RoD rigid. Surprisingly, we discover that whether global SA-RoD rigidity is a generic property of the underlying graph strongly depends on bipartitions of the vertex set, while infinitesimal SA-RoD rigidity and SA-RoD rigidity are generic properties (Theorem 8).

2) To discuss the effects of bipartitions on the SA-RoD rigidity property of frameworks, we introduce the connectivity of SA or RoD constraints (see Definition 2.4). It is proved that an SA-RoD constrained framework can inherit the global rigidity property of the pure SA or RoD constrained framework when SA or RoD constraints are connected (Theorem 3, Theorem 4). In addition, a novel duality is shown to hold for infinitesimal SA-RoD rigidity of frameworks associated with bipartitions (Theorem 6).

3) Based on the SA-RoD rigidity theory, vertex additions and merging operations are proposed to construct globally SA-RoD rigid frameworks. In contrast to that three edges are required to be added for merging bearing rigid frameworks in $\mathbb{R}^2$ [35], adding two edges appropriately when merging two globally SA-RoD rigid frameworks is sufficient to preserve global rigidity (Theorem 10). We show that frameworks generated by SA-RoD orderings are globally SA-RoD rigid (Theorem 9). Furthermore, we construct minimal SA-RoD rigid frameworks with n vertices and $\frac{3n-4}{2}$ edges (n is even) or $\frac{3n-3}{2}$ edges (n is odd). The number of edges required to guarantee rigidity of frameworks is fewer than those in pure SA/RoD rigidity theory [16, 14] and angle-displacement rigidity theory [29].

4) Necessary and sufficient conditions for network localizability are established. SA-RoD-based SNL is transformed into an edge-based problem, where distances and lengths of all edges are variables to be localized. Under the assumption of connected SA/RoD constraints, it can be reduced to two subproblems of finding distances and bearings, respectively (Algorithm 3, Algorithm 4). In particular, if the SA index set is connected over the underlying graph, the problem corresponds to solving a linear equation (Theorem 14). If both the SA index set and the RoD index set are disconnected, it can be transformed into a polynomial equation on a space whose dimension depends on the number of connected components (Algorithm 5, Theorem 17).

The remainder of this paper is organized as follows. Section 2 introduces SA-RoD rigidity theory, including the effects of bipartitions, shape uniqueness, generic property and construction of globally SA-RoD rigid frameworks. Section 3 formulates the SA-RoD-based SNL problem. An edge-based analysis via graph cycle basis is performed. Furthermore, localization algorithms are discussed according to the connectivity of constraints. Section 4 provides some simulating examples. Section 5 ends this article with conclusions and some suggestions on future work.

Notations: In this paper, $\mathbb{R}$ represents the set of real numbers; $\mathbb{C}$ is the set of complex numbers; $I_N \in \mathbb{R}^{N\times N}$ is the unit matrix; $\mathbb{R}^N$ denotes the vector space of dimension N; For a set T, $|T|$ denotes the number of elements in T; The norm of $x = (x_1, ..., x_n)^\top \in \mathbb{R}^n$ is denoted by $||x|| \triangleq [\sum_{k=1}^{n} x_k^2]^{\frac{1}{2}}$; for a matrix $X \in \mathbb{R}^{M\times N}$, the null space and rank of X are denoted by null(X) and rank(X), respectively; $X^\top$ denotes its transpose; $\mathbf{1}_n \triangleq (1, \cdots, 1)^\top \in \mathbb{R}^n$; For a square matrix $X \in \mathbb{R}^{N\times N}$, its determinant is denoted by $\det(X)$; $\otimes$ is the Kroneck product; $\odot$ is the Khatri-Rao product; $\mathcal{R}(\theta) \in \mathbb{R}^{2\times 2}$ is the rotation matrix associated with $\theta \in [0, 2\pi)$. We assume that $\mathcal{G} = (\mathcal{V}, \mathcal{E})$ is an undirected graph, where $\mathcal{V} = \{1, 2, \cdots, n\}$ is the vertex set, $\mathcal{E} \subseteq \mathcal{V} \times \mathcal{V}$ is the edge set with m edges. For vertex $i \in \mathcal{V}$, $\deg(i)$ is the degree of vertex i, and $\mathcal{N}_i \triangleq \{j \in \mathcal{V} : (j, i) \in \mathcal{E}\}$ is the set of neighbors of vertex i in graph $\mathcal{G}$. A complete graph with n vertices is denoted by $\mathcal{K}_n$. If the number of vertices is irrelevant, we simply denote it by $\mathcal{K}$. Δijk denotes the triangle with vertices i, j, k, while $\Diamond ijkl$ denotes the quadrilateral with vertices i, j, k, l. For a given graph $\mathcal{G}$ with an orientation, $H = [h_{ij}] \in \mathbb{R}^{m \times n}$ represents the incidence matrix with rows and columns indexed by edges and vertices of $\mathcal{G}$.

2 SA-RoD rigidity theory

In this section, we will define some concepts concerning SA-RoD rigidity. Based on these definitions, the effects of bipartitions of the vertex set, the shape uniqueness problem and generic properties of the defined rigidity concepts will be studied. Furthermore, construction approaches of globally SA-RoD rigid frameworks will be proposed.

Rigidity theories based on pure constraints such as distances, bearings, RoDs, and SAs are briefly introduced in Appendix A. Throughout the paper, $(\mathcal{G}(A, D), p)$ is used to represent the hybrid framework, where $\mathcal{G}(A, D) = (\mathcal{V}_A \cup \mathcal{V}_D, \mathcal{E})$ is the underlying graph with a bipartition $\mathcal{V} = \mathcal{V}_A \cup \mathcal{V}_D$, $|\mathcal{V}| = n \geq 3$, and $|\mathcal{E}| = m$, $p = [p_1^\top, p_2^\top, \cdots p_n^\top]^\top \in \mathbb{R}^{2n}$ is a configuration. Then, the triplet sets $\mathcal{T}_A, \mathcal{T}_D, \mathcal{T}_\mathcal{G}$, and $\mathcal{T}_\mathcal{K}$ are denoted by $\mathcal{T}_A = \{(u, v, w) \in \mathcal{V}^3 : u \in \mathcal{V}_A, (u, v), (u, w) \in \mathcal{E}, v < w\}$, $\mathcal{T}_D = \{(u, v, w) \in \mathcal{V}^3 : u \in \mathcal{V}_D, (u, v), (u, w) \in \mathcal{E}, v < w\}$, $\mathcal{T}_\mathcal{G} = \mathcal{T}_A \cup \mathcal{T}_D$, and $\mathcal{T}_\mathcal{K} = \{(u, v, w) \in \mathcal{V}^3 : v < w\}$. For $(r, s, t) \in \mathcal{T}_A$ and $(i, j, k) \in \mathcal{T}_D$, α_{rst} is the SA defined by (41) , and $\kappa_{ijk} = \frac{||p_k - p_i||}{||p_j - p_i||}$ is the RoD defined by (38) (with $l = 1$). Before introducing related notions, the following assumptions are given.

Assumption 1: Different nodes in the framework are not collocated.

Assumption 2: $\mathcal{V}_A \cap \mathcal{V}_D = \emptyset, \mathcal{V}_A \neq \emptyset, \mathcal{V}_D \neq \emptyset$.

Assumption 1 is commonly used in literature concerning rigidity theory and localization problems. From Assumption 2, we know that $\mathcal{V}_D$ and $\mathcal{V}_A$ are non-empty and constitute a non-trivial partition of the vertex set $\mathcal{V}$. Furthermore, $\mathcal{T}_A \neq \emptyset$, $\mathcal{T}_D \neq \emptyset$, and $\mathcal{T}_A \cap \mathcal{T}_D = \emptyset$. All the results in this work will be established under Assumption 1 and Assumption 2. For clarity, two vertices are said to have the same attributes if they belong to the same part of the bipartition ($\mathcal{V}_A$ or $\mathcal{V}_D$). To reveal the differences with pure SA or RoD rigidity, we start with a motivating example.

A motivating example: Consider non-degenerate quadrilateral frameworks as shown in Figure 1. Observe that the quadrilateral framework is neither RoD rigid nor SA rigid since there exist nontrivial deformations preserving RoD or SA constraints as plotted in Figures 1(a) and 1(b). When $\mathcal{V}_A = \{1\}$ as shown in Figure 1(c), there exists a flipping ambiguity for node 3. Similar results hold for frameworks in Figures 1(d) and 1(e). However, the shape of a quadrilateral framework constrained by SAs and RoDs as illustrated in Figure 1(f) can be uniquely determined up to uniform rotations, translations, and scalings as long as three nodes in $\mathcal{V}_A$ are non-collinear. This simple example indicates that mixing SA and RoD perceptions appropriately can guarantee the shape uniqueness even if it is neither RoD rigid nor SA rigid.

We will introduce definitions in SA-RoD rigidity theory that are analogous to those in distance

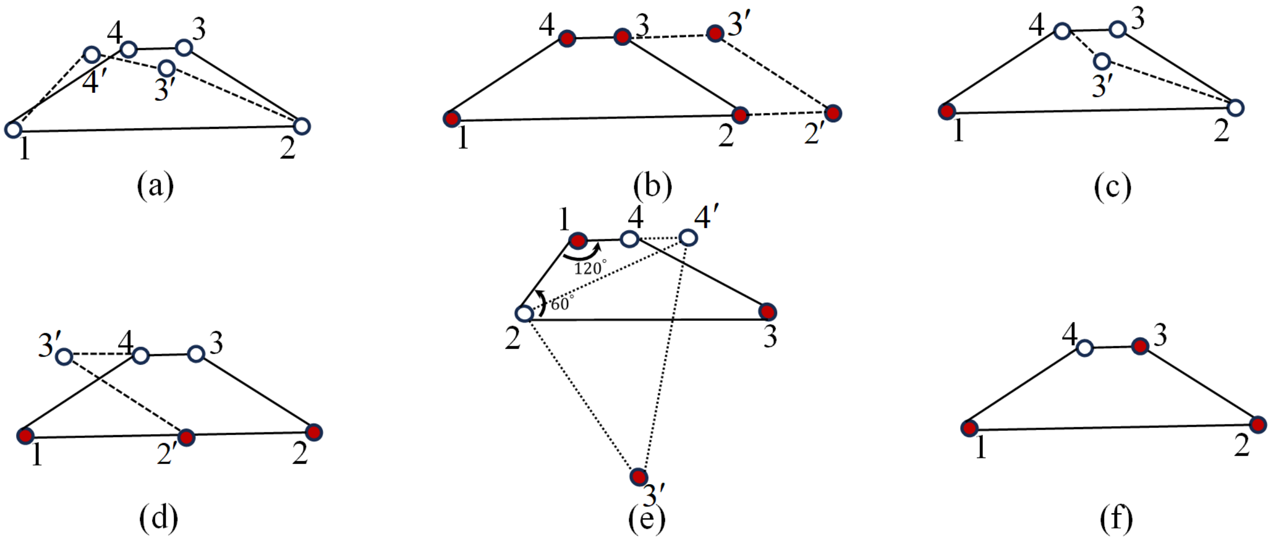

Fig. 1. Examples of quadrilateral frameworks. The dots in red represent nodes in $\mathcal{V}_A$, while hollow dots represent nodes in $\mathcal{V}_D$. (a) A pure RoD constrained framework that is not infinitesimally RoD rigid. (b) A pure SA constrained framework that is not infinitesimally SA rigid. (c) A framework with $\mathcal{V}_A = \{1\}$ whose shape can not be uniquely determined under the given bipartition. (d) A framework with $\mathcal{V}_A = \{1, 2\}$ whose shape can not be uniquely determined under the given bipartition. The coordinates of nodes $1, 2, 3, 4, 2', 3'$ are $(0, 0), (4, 0), (3, 1), (2, 1), (2, 0), (1, 1)$, respectively. (e) A framework with with $\mathcal{V}_A = \{1, 3\}$ whose shape can not be uniquely determined under the given bipartition. The coordinates of nodes $1, 2, 3, 4, 3', 4'$ are $(1, \sqrt{3}), (0, 0), (4, 0), (2, \sqrt{3}), (2, -2\sqrt{3}), (3, \sqrt{3})$, respectively. (f) A framework with $\mathcal{V}_A = \{1, 2, 3\}$ whose shape can be uniquely determined under the given bipartition.

rigidity theory. The SA-RoD rigidity function is defined as

$$f_{\mathcal{G}(A,D)}(p) \triangleq [\cdots, \alpha_{rst}, \cdots, \kappa_{ijk}, \cdots]^\top \in \mathbb{R}^{|\mathcal{T}_\mathcal{G}|},\ (r,s,t) \in \mathcal{T}_A,\ (i,j,k) \in \mathcal{T}_D. \tag{1}$$

Definition 2.1. A framework $(\mathcal{G}(A,D), p)$ is said to be SA-RoD rigid if there exists an open neighborhood U_p of p such that

$$f^{-1}_{\mathcal{G}(A,D)}(f_{\mathcal{G}(A,D)}(p)) \cap U_p = f^{-1}_{\mathcal{K}(A,D)}(f_{\mathcal{K}(A,D)}(p)) \cap U_p.$$

Otherwise, it is said to be flexible. $(\mathcal{G}(A,D), p)$ is called globally SA-RoD rigid if

$$f^{-1}_{\mathcal{G}(A,D)}(f_{\mathcal{G}(A,D)}(p)) = f^{-1}_{\mathcal{K}(A,D)}(f_{\mathcal{K}(A,D)}(p)).$$

The SA-RoD rigidity matrix is defined as

$$R_{\mathcal{G}(A,D)}(p) \triangleq \frac{\partial f_{\mathcal{G}(A,D)}(p)}{\partial p} \in \mathbb{R}^{|\mathcal{T}_\mathcal{G}| \times n}. \tag{2}$$

The infinitesimal SA-RoD motion refers to the motion δp maintaining the rigidity function $f_{\mathcal{G}(A,D)}(p)$, i.e.,

$$\dot{f}_{\mathcal{G}(A,D)}(p) = \frac{\partial f_{\mathcal{G}(A,D)}}{\partial p} \delta p = R_{\mathcal{G}(A,D)}(p)\delta p = 0, \tag{3}$$

where $\delta p = [\delta p_1^\top, \delta p_2^\top, \cdots, \delta p_n^\top]^\top,\ \delta p_i = \dot{p}_i$ is the velocity of node p_i. Note that uniform rotations, translations, and scalings always preserve the SA-RoD constraints of a framework. Therefore, an infinitesimal SA-RoD motion is said to be trivial if it corresponds to a combination of uniform translations, rotations and scalings of the framework. According to Lemma 3.1 in [13], the dimension of the trivial SA-RoD infinitesimal motion space in $\mathbb{R}^2$ is 4.

Definition 2.2. A framework $(\mathcal{G}(A,D), p)$ is said to be infinitesimally SA-RoD rigid if all infinitesimal SA-RoD motions of the framework are trivial.

To obtain a concise form of the rigidity matrix, let $e_{ij} = p_j - p_i,\ b_{ij} = \frac{e_{ij}}{||e_{ij}||}$. For derivatives of SA, we have [15]

$$\dot{\alpha}_{rst} = -[\frac{b_{rs}}{||e_{rs}||} - \frac{b_{rt}}{||e_{rt}||}]^\top \mathcal{R}(\pi/2)\dot{p}_r + \frac{b_{rs}^\top}{||e_{rs}||}\mathcal{R}(\pi/2)\dot{p}_s - \frac{b_{rt}^\top}{||e_{rt}||}\mathcal{R}(\pi/2)\dot{p}_t, (r,s,t) \in \mathcal{T}_A. \tag{4}$$

A direct calculation on derivatives of RoD provides that

$$\dot{\kappa}_{ijk} = \kappa_{ijk}\{[\frac{b_{ij}}{||e_{ij}||} - \frac{b_{ik}}{||e_{ik}||}]^\top \dot{p}_i - \frac{b_{ij}^\top}{||e_{ij}||}\dot{p}_j + \frac{b_{ik}^\top}{||e_{ik}||}\dot{p}_k\},\ (i,j,k) \in \mathcal{T}_D. \tag{5}$$

We can derive the following proposition by a similar proof of Lemma 1 in [15].

Proposition 1. *The SA-RoD rigidity matrix $R_{\mathcal{G}(A,D)}(p)$ can be expressed as*

$$R_{\mathcal{G}(A,D)}(p) = [\bar{R}_A^\top(p), \bar{R}_D^\top(p)]^\top \bar{H}, \tag{6}$$

where $\bar{H} = H \otimes I_2$*,* $\bar{R}_A(p) \in \mathbb{R}^{|\mathcal{T}_A| \times 2|\mathcal{E}|}$ *and* $\bar{R}_D(p) \in \mathbb{R}^{|\mathcal{T}_D| \times 2|\mathcal{E}|}$ *can be written as*

$$\begin{array}{cc} & \begin{array}{ccccc} \cdots & b_{rs} & \cdots & b_{rt} & \cdots \end{array} \\ \begin{array}{c} \cdots \\ \alpha_{rst} \\ \cdots \end{array} & \begin{pmatrix} \cdots & \cdots & \cdots & \cdots & \cdots \\ \mathbf{0} & \frac{b_{rs}^\top \mathcal{R}(\frac{\pi}{2})}{||e_{rs}||} & \mathbf{0} & -\frac{b_{rt}^\top \mathcal{R}(\frac{\pi}{2})}{||e_{rt}||} & \mathbf{0} \\ \cdots & \cdots & \cdots & \cdots & \cdots \end{pmatrix} \end{array}, \tag{7}$$

$$\begin{array}{cc} & \begin{array}{ccccc} \cdots & b_{ij} & \cdots & b_{ik} & \cdots \end{array} \\ \begin{array}{c} \cdots \\ \kappa_{ijk} \\ \cdots \end{array} & \begin{pmatrix} \cdots & \cdots & \cdots & \cdots & \cdots \\ \mathbf{0} & -\kappa_{ijk} \frac{b_{ij}^\top}{||e_{ij}||} & \mathbf{0} & \kappa_{ijk} \frac{b_{ik}^\top}{||e_{ik}||} & \mathbf{0} \\ \cdots & \cdots & \cdots & \cdots & \cdots \end{pmatrix} \end{array}. \tag{8}$$

All triplets corresponding to node i are subject to constraints induced by the sets $\mathcal{T}_A$ or $\mathcal{T}_D$. Nevertheless, we stress that a considerable degree of redundancy is present in these quantities. This is owing to a fundamental observation: for any $j, k, l \in \mathcal{N}_i$ satisfying $j < k < l$, it always holds that $\alpha_{ijk} + \alpha_{ikl} = \alpha_{ijl}, \kappa_{ijk}\kappa_{ikl} = \kappa_{ijl}$.

Lemma 1. $\mathrm{rank}(R_{\mathcal{G}(A,D)}(p)) \leq 2m - n$*.*

The proof is presented in Appendix B. The following equivalent characterizations of infinitesimal SA-RoD rigidity can be established.

Theorem 1. *Given a framework* $(\mathcal{G}(A, D), p)$*, then the following statements are equivalent:*
1) $(\mathcal{G}(A, D), p)$ *is infinitesimally SA-RoD rigid;*
2) $\mathrm{rank}(R_{\mathcal{G}(A,D)}(p)) = 2n - 4$*;*
3) $\mathrm{null}(R_{\mathcal{G}(A,D)}(p)) = \mathrm{span}\{\mathbf{1}_n \otimes I_2, (I_n \otimes \mathcal{R}(\pi/2))p, p\}$*.*

The proof is similar to that in [36, 14, 13]. Here we revisit frameworks in Figure 1. Frameworks in Figures 1(c), 1(d), and 1(e) are (infinitesimally) SA-RoD rigid but not globally SA-RoD rigid. In Figure 1(d), quadrilaterals $\lozenge 1234$ and $\lozenge 12'3'4$ are (infinitesimally) SA-RoD rigid but not globally SA-RoD rigid. In Figure 1(e), quadrilaterals $\lozenge 1234$ and $\lozenge 123'4'$ are (infinitesimally) SA-RoD rigid but not globally SA-RoD rigid. The framework in Figure 1(f) is both (infinitesimally) SA-RoD rigid and globally SA-RoD rigid.

Figure 2 also presents some SA-RoD constrained frameworks. We can see that even a degenerate triangle can become globally SA-RoD rigid. A quadrilateral is also globally SA-RoD rigid if $|\mathcal{V}_D| = 1$ and three nodes in $\mathcal{V}_A$ are non-collinear. Figure 2(c) provides a quadrilateral with collinear four nodes. Due to the collinearity, global rigidity can be derived from RoD constraints $\kappa_{213}, \kappa_{324}, \kappa_{413}$ and SA constraint α_{124}. The framework in Figure 2(d) is infinitesimally SA-RoD rigid but not globally SA-RoD rigid. There exists a reflection of node 5 with respect to the line connecting nodes 1 and 4, which can preserve the SA-RoD constraints.

To investigate the relationships among infinitesimal SA-RoD rigidity, SA-RoD rigidity, and global SA-RoD rigidity for general frameworks, our analysis starts with $(\mathcal{K}(A, D), p)$. For a given configuration $p \in \mathbb{R}^{2n}$ satisfying Assumption 1, the set S_p of configurations with the same shape as p up to

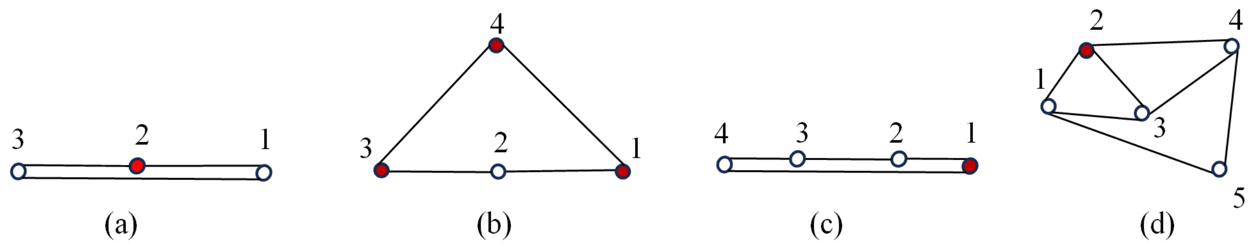

Fig. 2. (a) A globally and infinitesimally SA-RoD rigid framework corresponding to a degenerate triangle with $\mathcal{V}_A = \{2\}$. (b) A globally and infinitesimally SA-RoD rigid framework corresponding to a quadrilateral with $\mathcal{V}_A = \{1, 3, 4\}$. (c) A globally SA-RoD rigid framework that is not infinitesimally SA-RoD rigid corresponding to a degenerate quadrilateral with $\mathcal{V}_A = \{1\}$. (d) An infinitesimally SA-RoD rigid framework that is not globally SA-RoD rigid on a Laman graph with $\mathcal{V}_A = \{2\}$. The dots in red represent nodes in $\mathcal{V}_A$.

uniform rotations, translations, and scalings is defined as

$$S_p \triangleq \{q \in \mathbb{R}^{2n} : q = \mathbf{1}_n \otimes \xi + c(I_n \otimes \mathcal{R}(\theta))p, \xi \in \mathbb{R}^2, \theta \in [0, 2\pi), c \in \mathbb{R}^+\}. \tag{9}$$

It is noteworthy that an equivalent definition of S_p permits $c \in \mathbb{R} - \{0\}$. The restriction of c to positive values is imposed to ensure the uniqueness of parameters c, θ. Specifically, given any $q \in S_p$, parameters $c > 0$ and $\theta \in [0, 2\pi)$ satisfying $q = \mathbf{1}_n \otimes \xi + c(I_n \otimes \mathcal{R}(\theta))p$ are unique.

Lemma 2. *For a complete graph $\mathcal{K}(A, D)$ with a bipartition and a configuration $p \in \mathbb{R}^{2n}$, it holds that $f^{-1}_{\mathcal{K}(A,D)}(f_{\mathcal{K}(A,D)}(p)) = S_p$.*

The proof of Lemma 2 is presented in Appendix C. If $p \in \mathbb{R}^{2n}$ is non-degenerate, it is well known that S_p is a smooth manifold with dimension 4. Here we show that under Assumption 1, this property still holds even if p is degenerate. We provide the detailed proof in Appendix D.

Lemma 3. *S_p is a 4-dimensional smooth manifold and is diffeomorphic to $\mathbb{S}^1 \times \mathbb{R}^2 \times \mathbb{R}^+$.*

With the aid of Lemma 2 and Lemma 3, we can derive the following relationship between infinitesimal SA-RoD rigidity and SA-RoD rigidity.

Theorem 2. *If a framework $(\mathcal{G}(A, D), p)$ is infinitesimally SA-RoD rigid, it is SA-RoD rigid.*

Proof. Based on the infinitesimal SA-RoD rigidity of $(\mathcal{G}(A, D), p)$, it holds that $\text{rank}(R_{\mathcal{G}(A,D)}(p))) = 2n-4$. According to Proposition 2 in [36], there exists a neighborhood U of p such that $f^{-1}_{\mathcal{G}(A,D)}(f_{\mathcal{G}(A,D)}(p)) \cap U$ is a 4-dimensional manifold. Combining Lemma 2 and Lemma 3, $f^{-1}_{\mathcal{K}(A,D)}(f_{\mathcal{K}(A,D)}(p)) \cap U = S_p \cap U$ is a 4-dimensional manifold. Since $f^{-1}_{\mathcal{K}(A,D)}(f_{\mathcal{K}(A,D)}(p)) \subseteq f^{-1}_{\mathcal{G}(A,D)}(f_{\mathcal{G}(A,D)}(p))$, we can conclude that $f^{-1}_{\mathcal{K}(A,D)}(f_{\mathcal{K}(A,D)}(p)) \cap U = f^{-1}_{\mathcal{G}(A,D)}(f_{\mathcal{G}(A,D)}(p)) \cap U$. Therefore, $(\mathcal{G}(A, D), p)$ is SA-RoD rigid. □

Note that the converse of this theorem is not true. Figure 2(c) presents a framework that is globally SA-RoD rigid, but not infinitesimally SA-RoD rigid. By definition, global SA-RoD rigidity of a framework implies SA-RoD rigidity. Furthermore, the example in Figure 2(d) indicates that there exist frameworks that are SA-RoD rigid, but not globally SA-RoD rigid.

2.1 Bipartition of the vertex set

As shown in the motivating example, bipartitions of the vertex set have significant effects on the rigidity property of corresponding frameworks. Given the underlying graph $\mathcal{G} = (\mathcal{V}, \mathcal{E})$ and a configuration $p \in \mathbb{R}^{2n}$, there are some natural questions related to possible bipartitions: 1) Are there any non-trivial bipartitions of the vertex set such that the associated framework $(\mathcal{G}(A, D), p)$ is infinitesimally/globally SA-RoD rigid? If a framework is globally SA rigid or RoD rigid, how to construct suitable bipartitions to guarantee global SA-RoD rigidity? 2) Are there any intrinsic relationships among (global) SA-RoD rigidities under different bipartitions of the vertex set?

2.1.1 Inherent properties under connectivity constraints

In this subsection, we will introduce the defintions of the SA (RoD) index graph and the connectivity analogously to those in [15]. Based on these definitions, we can answer question 1) by showing that framework $(\mathcal{G}(A, D), p)$ can inherit the SA or RoD rigidity property of framework $(\mathcal{G}, p)$ under the assumption of connectivity.

We first introduce the following definition of the triple index graph.

Definition 2.3 (Triple index graph)**.** For a graph $\mathcal{G}$ and a triple index set $\hat{\mathcal{T}}_{\mathcal{G}} \subseteq \mathcal{T}_{\mathcal{G}}$, the undirected triple index graph is denoted by $\mathcal{G}_T(\hat{\mathcal{T}}_{\mathcal{G}}) = (\mathcal{V}_T(\mathcal{G}), \mathcal{E}_T(\hat{\mathcal{T}}_{\mathcal{G}}))$, where the vertex set is $\mathcal{V}_T(\mathcal{G}) = \{a_{ij} = H(i, j, |\mathcal{V}|) : (i, j) \in \mathcal{E}\}$, $H(i, j, \mathcal{V}) = (\min\{i, j\} - 1) \times |\mathcal{V}| + \max(\{i, j\})$, and the edge set is $\mathcal{E}_T(\hat{\mathcal{T}}_{\mathcal{G}}) = \{(a_{ji}, a_{jk}) : a_{ji}, a_{jk} \in \mathcal{V}_T(\mathcal{G}), (i, j, k) \in \hat{T}_{\mathcal{G}}\}$.

The expression of H in above definition indicates that $a_{ij} = a_{ji},\ (i, j) \in \mathcal{E}$. Thus, we know that $a_{ij} \in \mathcal{V}_T(\mathcal{G})$ if and only if $a_{ji} \in \mathcal{V}_T(\mathcal{G})$. Based on Definition 2.3, we introduce the definition of the SA or RoD connectivity as follows.

Definition 2.4 (SA or RoD connectivity)**.** For a graph $\mathcal{G}$ and a triple SA (RoD) index set $\mathcal{T}_A \subseteq \mathcal{T}_{\mathcal{G}}$ ($\mathcal{T}_D \subseteq \mathcal{T}_{\mathcal{G}}$), $\mathcal{T}_A$ ($\mathcal{T}_D$) is said to be connected over $\mathcal{G}$ if the corresponding undirected triple index graph $\mathcal{G}_T(\mathcal{T}_A)$ ($\mathcal{G}_T(\mathcal{T}_D)$) is connected. Moreover, $\mathcal{T}_A$ ($\mathcal{T}_D$) is said to have c connected components over $\mathcal{G}$ if $\mathcal{G}_T(\mathcal{T}_A)$ ($\mathcal{G}_T(\mathcal{T}_D)$) has c connected components.

Figure 3 presents a graph with a given bipartition, the SA index graph, and the RoD index graph. According to two definitions above, $\mathcal{T}_A$ has five connected components, and $\mathcal{T}_D$ is connected over $\mathcal{G}$.

Definition 2.5 (Global index set)**.** For a given framework $\mathcal{G}(A, D), p)$, the triple SA (RoD) index set $\mathcal{T}_A \subseteq \mathcal{T}_{\mathcal{G}}$ ($\mathcal{T}_D \subseteq \mathcal{T}_{\mathcal{G}}$) is called a global SA (RoD) index set if for any configuration $q \in \mathbb{R}^{2n}$ satisfying $\alpha_{ijk}(q) = \alpha_{ijk}(p),\ (i, j, k) \in \mathcal{T}_A$ ($\kappa_{ijk}(q) = \kappa_{ijk}(p),\ (i, j, k) \in \mathcal{T}_D$), it holds that $\alpha_{ijk}(q) = \alpha_{ijk}(p)$ ($\kappa_{ijk}(q) = \kappa_{ijk}(p)$) for all $(i, j, k) \in \mathcal{T}_{\mathcal{G}}$.

Following the same routine to prove Lemma 6 in [15], we can show that the connectivity of a RoD index set also implies it is a global RoD index set. These results can be summarized as follows.

Lemma 4. *For a framework $(\mathcal{G}(A, D), p)$ in $\mathbb{R}^2$, the SA (RoD) index set $\mathcal{T}_A$ ($\mathcal{T}_D$) is a global SA (RoD) index set if it is connected over $\mathcal{G}$.*

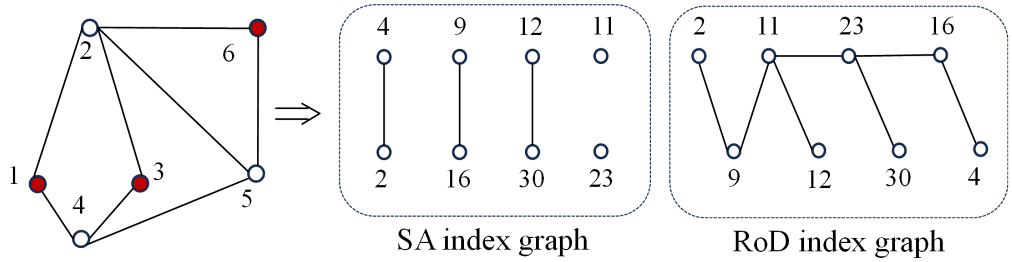

Fig. 3. An example of a graph associated with a given bipartition, the SA index graph, and the RoD index graph. There exist five connected components in the SA index graph, while the RoD index graph is connected. The dots in red represent nodes in $\mathcal{V}_A$. The vertices in SA/RoD index graphs satisfy $2 = a_{12}, 4 = a_{14}, 9 = a_{23}, 11 = a_{25}, 12 = a_{26}, 16 = a_{34}, 23 = a_{45}, 30 = a_{56}$.

If the SA index set associated with a bipartition of the vertex set is global, we present the following theorem.

Theorem 3. *For an infinitesimally SA rigid framework $(\mathcal{G}, p)$ in $\mathbb{R}^2$, and a given partition $\mathcal{V} = \mathcal{V}_A \cup \mathcal{V}_D$, if the SA index set $\mathcal{T}_A$ is connected over $\mathcal{G}$, then $(\mathcal{G}(A, D), p)$ is globally SA-RoD rigid.*

Proof. Suppose $q \in f^{-1}_{\mathcal{G}(A,D)}(f_{\mathcal{G}(A,D)}(p))$, then $\alpha_{ijk}(q) = \alpha_{ijk}(p)$ for $(i, j, k) \in \mathcal{T}_A$. According to Lemma 4, $\mathcal{T}_A$ is a global SA index set. By Definition 2.5, it holds that $\alpha_{ijk}(q) = \alpha_{ijk}(p)$ for $(i, j, k) \in \mathcal{T}_{\mathcal{G}}$. Based on Lemma 13, infinitesimal SA rigidity of $(\mathcal{G}, p)$ implies that SA constraints induced by $\mathcal{T}_{\mathcal{G}}$ are sufficient to guarantee the shape uniqueness. Thus, the shape of $(\mathcal{G}(A, D), p)$ can be uniquely determined by SA constraints in $\mathcal{T}_A$. From Theorem 7 (its proof is self-contained), $(\mathcal{G}(A, D), p)$ is globally SA-RoD rigid. □

Remark 1. *Based on Lemma* 13*, we know that the result in Theorem* 3 *is also valid for non-degenerate and globally SA rigid frameworks.*

Similarly, if $(\mathcal{G}, p)$ is globally RoD rigid, we can show that $(\mathcal{G}(A, D), p)$ can inherit the rigidity property when the RoD index set $\mathcal{T}_D$ is connected over $\mathcal{G}$.

Theorem 4. *For a globally RoD rigid framework $(\mathcal{G}, p)$ in $\mathbb{R}^2$, and a given partition $\mathcal{V} = \mathcal{V}_A \cup \mathcal{V}_D$, if the RoD index set $\mathcal{T}_D$ is connected over $\mathcal{G}$, then $(\mathcal{G}(A, D), p)$ is globally SA-RoD rigid as well.*

Remark 2. *According to Lemma* 11*, we know the conlusion is still valid for globally distance rigid frameworks in $\mathbb{R}^2$. In distance rigidity theory, it has been shown that $\mathcal{G}$ is globally rigid in $\mathbb{R}^2$ if and only if either $\mathcal{G}$ is a complete graph on at most three vertices or $\mathcal{G}$ is 3-connected and redundantly rigid [37].*

2.1.2 Duality

Concerning question 2), we present a novel duality of infinitesimal SA-RoD rigidity with respect to two bipartitions.

Theorem 5 (Dual rank property)**.** *Given two frameworks* $(\mathcal{G}(A,D),p) = (\mathcal{V}_A \cup \mathcal{V}_D, \mathcal{E}, p)$ *and* $(\mathcal{G}'(A,D),p) = (\mathcal{V}'_A \cup \mathcal{V}'_D, \mathcal{E}', p)$*. If* $\mathcal{V}'_D = \mathcal{V}_A, \mathcal{V}'_A = \mathcal{V}_D$*, and* $\mathcal{E}' = \mathcal{E}$*, then* $\mathrm{rank}(R_{\mathcal{G}(A,D)}(p)) = \mathrm{rank}(R_{\mathcal{G}'(A,D)}(p))$.

The proof can be found in Appendix E. According to the defintion of infinitesimal SA-RoD rigidity, we can derive the following duality theorem.

Theorem 6 (Duality of infinitesimal SA-RoD rigidity)**.** *Given two frameworks* $(\mathcal{G}(A,D),p) = (\mathcal{V}_A \cup \mathcal{V}_D, \mathcal{E}, p)$ *and* $(\mathcal{G}'(A,D),p) = (\mathcal{V}'_A \cup \mathcal{V}'_D,\ \mathcal{E}', p)$*. If* $\mathcal{V}'_D = \mathcal{V}_A,\ \mathcal{V}'_A = \mathcal{V}_D$*, and* $\mathcal{E}' = \mathcal{E}$*, then* $(\mathcal{G}(A,D),p)$ *is infinitesimally SA-RoD rigid if and only if* $(\mathcal{G}'(A,D),p)$ *is infinitesimally SA-RoD rigid.*

Remark 3. *In fact, our proof still holds for* $\mathcal{V}_A = \emptyset$ *or* $\mathcal{V}_D = \emptyset$*. As a byproduct, we can show that the SA rigidity matrix and RoD rigidity matrix of a given framework have the same rank. Therefore, in* $\mathbb{R}^2$*, infinitesimal SA rigidity is equivalent to infinitesimal RoD rigidity. This can also be obtained by the results in [15, 16]. However, as illustrated in Figure* 2(*a*)*, infinitesimal SA-RoD rigidity of a framework is not equivalent to infinitesimal SA rigidity or infinitesimal RoD rigidity.*

It is worth noting that this duality is lacking for SA-RoD rigidity and global SA-RoD rigidity. A typical example is provided by the degenerate quadrilateral in Figure 2(c). If $\mathcal{V}_A = \{1\}$ and $\mathcal{V}_D = \{2,3,4\}$, then $(\mathcal{G}(A,D),p)$ is globally SA-RoD rigid. If $\mathcal{V}_A$ and $\mathcal{V}_D$ are swapped, then the induced framework $(\mathcal{G}(A,D),p)$ is not SA-RoD rigid. The reason is that node 3 can move freely on the segment connecting node 2 and node 4. However, we can show that for a generic configuration p (see the definition in Appendix A.2), this duality holds for SA-RoD rigidity as a direct consequence of Lemma 16. A detailed discussion of generic properties will be given in Subsection 2.3.

Corollary 1 (Duality of SA-RoD rigidity)**.** *For frameworks* $(\mathcal{G}(A,D),p) = (\mathcal{V}_A \cup \mathcal{V}_D, \mathcal{E}, p)$ *and* $(\mathcal{G}'(A,D),p) = (\mathcal{V}'_A \cup \mathcal{V}'_D,\ \mathcal{E}', p)$*. If the configuration* p *is generic in* $\mathbb{R}^{2n}$*,* $\mathcal{V}'_D = \mathcal{V}_A,\ \mathcal{V}'_A = \mathcal{V}_D$*, and* $\mathcal{E}' = \mathcal{E}$*, then* $(\mathcal{G}(A,D),p)$ *is SA-RoD rigid if and only if* $(\mathcal{G}'(A,D),p)$ *is SA-RoD rigid.*

2.2 Shape determination

In this subsection, we investigate under what conditions the shape of a framework can be uniquely determined by SA and RoD constraints.

2.2.1 Characterizations of shape uniqueness

For a fixed configuration $p \in \mathbb{R}^{2n}$, the set S_p characterizes all configurations owning the same shape as p. Given a framework $(\mathcal{G}(A,D),p)$, the configuration set of frameworks satisfying the same SA and RoD constraints as $(\mathcal{G}(A,D),p)$ is $f^{-1}_{\mathcal{G}(A,D)}(f_{\mathcal{G}(A,D)}(p))$. Therefore, we can naturally derive the following lemma.

Lemma 5. *The shape of a framework* $(\mathcal{G}(A,D),p)$ *in* $\mathbb{R}^2$ *can be uniquely determined by SA and RoD constraints up to uniform rotations, translations, and scalings if and only if* $f^{-1}_{\mathcal{G}(A,D)}(f_{\mathcal{G}(A,D)}(p)) = S_p$.

Based on Lemma 5, we present the following theorem to characterize the shape uniqueness of frameworks under SA and RoD constraints.

Theorem 7. *For a given framework $(\mathcal{G}(A,D),p)$ in $\mathbb{R}^2$, the following statements are equivalent:*
1) $(\mathcal{G}(A,D),p)$ is globally SA-RoD rigid.
2) The shape of $(\mathcal{G}(A,D),p)$ can be uniquely determined by $\{\alpha_{ijk}:(i,j,k)\in\mathcal{T}_A\}$ and $\{\kappa_{ijk}:(i,j,k)\in\mathcal{T}_D\}$ up to uniform rotations, translations, and scalings.
3) All SAs in $\{\alpha_{ijk}:(i,j,k)\in\mathcal{T}_\mathcal{G}\}$ and RoDs in $\{\kappa_{ijk}:(i,j,k)\in\mathcal{T}_\mathcal{G}\}$ can be uniquely determined by $\{\alpha_{ijk}:(i,j,k)\in\mathcal{T}_A\}$ and $\{\kappa_{ijk}:(i,j,k)\in\mathcal{T}_D\}$.
4) All SAs in $\{\alpha_{ijk}:(i,j,k)\in\mathcal{T}_\mathcal{K}\}$ and RoDs in $\{\kappa_{ijk}:(i,j,k)\in\mathcal{T}_\mathcal{K}\}$ can be uniquely determined by $\{\alpha_{ijk}:(i,j,k)\in\mathcal{T}_A\}$ and $\{\kappa_{ijk}:(i,j,k)\in\mathcal{T}_D\}$..

Proof. Equivalence of 1) and 2): From Lemma 2, $f^{-1}_{\mathcal{K}(A,D)}(f_{\mathcal{K}(A,D)}(p))=S_p$. Utilizing Lemma 5, the shape of a framework $(\mathcal{G}(A,D),p)$ can be uniquely determined by SA and RoD constraints up to trivial infinitesimal motions if and only if $f^{-1}_{\mathcal{G}(A,D)}(f_{\mathcal{G}(A,D)}(p))=S_p=f^{-1}_{\mathcal{K}(A,D)}(f_{\mathcal{K}(A,D)}(p))$. This is equivalent to global SA-RoD rigidity.
Equivalence of 2) and 3): The argument is similar to that of Lemma 2.
Equivalence of 2) and 4): Observe that 2) implies 4), and 4) implies 3). Since 2) and 3) are equivalent, we obtain the desired equivalence of 2) and 4). □

Theorem 7 indicates the equivalence between global SA-RoD rigidity and shape uniqueness under SA and RoD constraints. In addition, it also provides an important perspective on global SA-RoD rigidity, analogous to the matrix completion in distance rigidity theory.

2.2.2 Shape uniqueness of quadrilaterals

Building on the aforementioned results, we deal with the shape determination problem of quadrilateral frameworks in this subsection. We mainly discuss whether all the SAs and RoDs of a quadrilateral can be uniquely determined by SA and RoD constraints under different bipartitions.

Given a quadrilateral framework $(\mathcal{G}(A,D),p)$ with $\mathcal{V}=\{1,2,3,4\}$ and $\mathcal{E}=\{(1,2),(2,3),(3,4),(4,1)\}$, we have

$$d_{12}b_{12}+d_{23}b_{23}+d_{34}b_{34}+d_{41}b_{41}=0, \tag{10}$$

where $d_{ij}=||p_i-p_j||>0$, $b_{ij}=\frac{p_j-p_i}{||p_j-p_i||}\in\mathbb{R}^2$. Denote $b_{ij}=[\cos\theta_{ij},\sin\theta_{ij}]^\top$, where $\theta_{ij}\in[0,2\pi),\ 1\leq i<j\leq 4$. Then, (10) can be rewritten as:

$$d_{12}\begin{bmatrix}\cos\theta_{12}\\ \sin\theta_{12}\end{bmatrix}+d_{23}\begin{bmatrix}\cos\theta_{23}\\ \sin\theta_{23}\end{bmatrix}+d_{34}\begin{bmatrix}\cos\theta_{34}\\ \sin\theta_{34}\end{bmatrix}+d_{41}\begin{bmatrix}\cos\theta_{41}\\ \sin\theta_{41}\end{bmatrix}=0, \tag{11}$$

According to bipartitions of the vertex set, global SA-RoD rigidity of a quadrilateral framework can be categorized into six cases as illustrated in Figure 1. Since purely SA or RoD constrained quadrilateral frameworks are well understood, the solutions to (11) in the remaining four cases are analyzed in Appendix *F*. In summary, we obtain the following criterion of global SA-RoD rigidity for quadrilateral frameworks.

Proposition 2. *A quadrilateral framework $(\mathcal{G}(A,D),p)$ with $\mathcal{V}=\{1,2,3,4\}$ and $\mathcal{E}=\{(1,2),(2,3),(3,4),(4,1)\}$ is globally SA-RoD rigid if and only if it satisfies one of the following conditions:*

1) $|\mathcal{V}_A| = 3, |\mathcal{V}_D| = 1$*, and nodes in* $\mathcal{V}_A$ *are non-collinear.*
2) $|\mathcal{V}_A| = 1, |\mathcal{V}_D| = 3$*, and either nodes* $2, 3$*, and* 4 *are collinear or* $d_{14} = d_{34}, d_{12} = d_{32}$*, where without loss of generality, assume that* $\mathcal{V}_A = \{1\}, \mathcal{V}_D = \{2, 3, 4\}$*.*
3) $|\mathcal{V}_A| = 2, |\mathcal{V}_D| = 2$*, nodes in* $\mathcal{V}_A$ *are adjacent and it holds that*

$$d_{12} + 2d_{34}\cos(\theta_{34} - \theta_{12}) \leq 0, \tag{12}$$

where without loss of generality, assume that $\mathcal{V}_A = \{1, 2\}, \mathcal{V}_D = \{3, 4\}$*.*
4) $|\mathcal{V}_A| = 2, |\mathcal{V}_D| = 2$*, nodes in* $\mathcal{V}_A$ *are not adjacent and it holds that*

$$d_{12}^2 d_{34}^2 + d_{14}^2 d_{23}^2 - d_{14}^2 d_{21}^2 \sin^2\theta_{124} - d_{34}^2 d_{23}^2 \sin^2\theta_{324} - 2d_{12}d_{23}d_{34}d_{14}\cos\theta_{324}\cos\theta_{124} = 0, \tag{13}$$

or

$$(d_{23} - d_{12})(d_{34} - d_{14}) \leq 0, \tag{14}$$

where without loss of generality, assume that $\mathcal{V}_A = \{1, 3\}, \mathcal{V}_D = \{2, 4\}$*,* $\theta_{324} = \theta_{34} - \theta_{32}$*, and* $\theta_{124} = \theta_{14} - \theta_{12}$*.*

This proposition provides useful criteria to check whether an SA-RoD constrained quadrilateral framework is globally rigid. It can serve as an essential unit to construct globally rigid frameworks and discuss generic properties of underlying graphs.

2.3 Generic property

This subsection focuses on the generic property of (infinitesimal/global) SA-RoD rigidity. We will prove that (infinitesimal) SA-RoD rigidity is a generic property of the underlying graph of a framework with a given bipartition of the vertex sets. Significantly different from bearing (or distance) rigidity theory, bipartitions can be critical to the generic property of global SA-RoD rigidity. To state these results, we first give a definition of generic SA-RoD rigidity for graphs.

Definition 2.6. A graph $\mathcal{G}(A, D)$ with a specific bipartition of the vertex set is called generically (infinitesimally) SA-RoD rigid in $\mathbb{R}^2$ if for any generic configuration $p \in \mathbb{R}^{2n}$, $(\mathcal{G}(A, D), p)$ is (infinitesimally) SA-RoD rigid.

Similar to the discussions of generic distance rigidity for graphs in [38], the following theorem shows that (infinitesimally) SA-RoD rigidity is a generic property of the underlying graph. The proof is provided in Appendix G.

Theorem 8. *Suppose for a given generic configuration* $p \in \mathbb{R}^{2n}$*,* $(\mathcal{G}(A, D), p)$ *is an (infinitesimally) SA-RoD rigid framework, then graph* $\mathcal{G} = (\mathcal{V}_A \cup \mathcal{V}_D, \mathcal{E})$ *is generically (infinitesimally) SA-RoD rigid.*

Next, we give a counterexample to show that bipartitions of the underlying graph can have a fundamental effect on the generic property of global SA-RoD rigidity.

A counterexample: For graph $\mathcal{G}(A, D)$ with a specific bipartition $\mathcal{V}_A = \{1, 2\}$, $\mathcal{V}_D = \{3, 4\}$, and $\mathcal{E} = \{(1, 2), (2, 3), (3, 4), (4, 1)\}$, let $(\mathcal{G}(A, D), p)$ be a quadrilateral framework as plotted in Figure

1(d). According to (12), the configuration set of globally SA-RoD rigid frameworks occupies a positive measure in $\mathbb{R}^8$. In addition, the complement set of globally SA-RoD rigid frameworks is characterized by $d_{12} + 2d_{34}\cos(\theta_{34} - \theta_{12}) > 0$, which also occupies a positive measure in $\mathbb{R}^8$. However, if global SA-RoD rigidity was a generic property of the underlying graph, either the configuration set of globally SA-RoD rigid frameworks or the complement set must have a zero measure. Therefore, under this setting, global SA-RoD rigidity is not a generic property for the underlying graph $\mathcal{G}(A, D)$ with the given bipartition.

However, if the bipartition is defined by $\mathcal{V}_A = \{1, 2, 3\}$ and $\mathcal{V}_D = \{4\}$, Proposition 2 indicates that global SA-RoD rigidity is a generic property for the underlying graph $\mathcal{G}(A, D)$ with this bipartition.

This counterexample reveals an important aspect that distinguishes the SA-RoD rigidity theory from existing pure rigidity theories. As a consequence, besides underlying graphs, the effects of configurations and bipartitions can not be neglected when constructing global SA-RoD rigid frameworks.

2.4 Combinatorial construction of globally SA-RoD rigid frameworks

In this section, we present some important operations to construct globally SA-RoD rigid frameworks. Since global SA-RoD rigidity may not be a generic property of a graph, our construction of globally SA-RoD rigid frameworks is based on frameworks, not graphs.

We first establish a lower bound on the number of edges required to guarantee SA-RoD rigidity.

Lemma 6. *Given a framework $(\mathcal{G}(A, D), p)$ in $\mathbb{R}^2$, if $(\mathcal{G}(A, D), p)$ is infinitesimally SA-RoD rigid, then $m \geq \frac{3n-4}{2}$.*

Proof. Suppose $m < \frac{3n-4}{2}$. By Lemma 1, the number of total independent constraints is upper-bounded by $2m - n < 2n - 4$. Therefore, $\mathrm{rank}(\frac{\partial f_{\mathcal{G}}}{\partial p}) < 2n - 4$. So $(\mathcal{G}(A, D), p)$ is not infinitesimally SA-RoD rigid. This leads to a contradiction. $\square$

According to Lemma 16, we know that the conclusion is also valid for an SA-RoD rigid framework with a generic configuration. In fact, the lower bound in Lemma 6 is tight. We will construct some (globally) SA-RoD rigid frameworks satisfying $m = \frac{3n-4}{2}$ when n is even or $m = \frac{3n-3}{2}$ when n is odd. Combining with Lemma 6, these frameworks are shown to be minimal. That is, after deleting any one edge, the (global) SA-RoD rigidity will be broken.

2.4.1 Vertex addition

To introduce the construction approach, classical vertex additions in Henneberg construction are modified here to maintain global SA-RoD rigidity. According to the constraints induced by newly added nodes, we give four types of 1-vertex additions as follows.

Definition 2.7. Given a framework $(\mathcal{G}(A, D), p)$ with $|\mathcal{V}| = n$, add a vertex $n + 1$ and two edges connecting vertex $n + 1$ with two existing vertices i, j. Let p_{n+1} be the coordinate of vertex $n + 1$ and denote $\mathcal{V}' = \mathcal{V} \cup \{n + 1\}$. Consider a bipartition $\mathcal{V}' = \mathcal{V}'_A \cup \mathcal{V}'_D$ such that $\mathcal{V}_A \subseteq \mathcal{V}'_A$ and $\mathcal{V}_D \subseteq \mathcal{V}'_D$, then the operation is called
1) a Type A_1 1-vertex addition if $n + 1 \in \mathcal{V}'_A$, and $i \in \mathcal{V}_D$ or $j \in \mathcal{V}_D$.

2) a Type D_1 1-vertex addition if $n+1 \in \mathcal{V}'_D$, and $i \in \mathcal{V}_A$ or $j \in \mathcal{V}_A$.
3) a Type A_2 1-vertex addition if $n+1 \in \mathcal{V}'_A$, $i, j \in \mathcal{V}_A$, and p_i, p_j, p_{n+1} are non-collinear.
4) a Type D_2 1-vertex addition if $n+1 \in \mathcal{V}'_D$, $i, j \in \mathcal{V}_D$, and for a third existing vertex $k \in \mathcal{V}_D$ such that p_i, p_j, and p_k are non-collinear, the third edge $(n+1, k)$ is added.

The four types of 1-vertex additions defined above are illustrated in Figure 4. After performing a Type A_1 1-vertex addition, we obtain an induced framework $(\mathcal{G}'(A, D), p')$ defined by

$$\mathcal{V}'_A \triangleq \mathcal{V}_A \cup \{n+1\}, \mathcal{V}'_D \triangleq \mathcal{V}_D, \mathcal{E}' \triangleq \mathcal{E} \cup \{(n+1, i), (n+1, j)\}, p' \triangleq [p^\top, p_{n+1}^\top]^\top \in \mathbb{R}^{2(n+1)}.$$

Similarly, frameworks induced by other types of 1-vertex additions can also be defined. Now we show

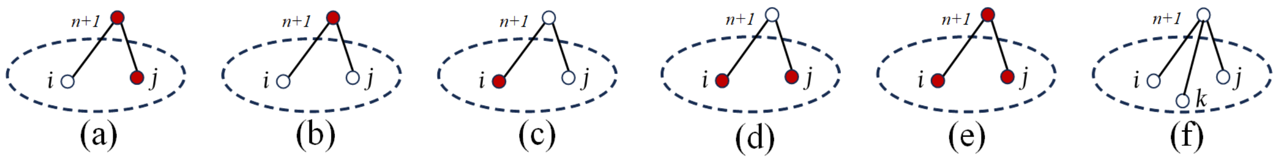

Fig. 4. Various types of 1-vertex additions. (a)(b) Type A_1 1-vertex addition. (c)(d) Type D_1 1-vertex addition. (e)Type A_2 1-vertex addition. (f) Type D_2 1-vertex addition. The dots in red represent nodes in $\mathcal{V}_A$.

that all types of 1-vertex additions can preserve the global SA-RoD rigidity if the original framework is globally SA-RoD rigid. The proof is provided in Appendix H.

Lemma 7. *Given a globally SA-RoD rigid framework $(\mathcal{G}(A, D), p)$ in $\mathbb{R}^2$, after performing a 1-vertex addition (including Type A_1, Type A_2, Type D_1, and Type D_2), the induced framework $(\mathcal{G}'(A, D), p')$ is globally SA-RoD rigid as well.*

To reduce the number of edges added during the construction, we can also employ 2-vertex additions to preserve global rigidity.

Definition 2.8. Given a framework $(\mathcal{G}(A, D), p)$ with $|\mathcal{V}| = n$, add two vertices $n+1, n+2$ and three edges $(j, n+1), (n+1, n+2), (n+2, i)$ connecting with two existing nodes i, j, denote $\mathcal{V}' = \mathcal{V} \cup \{n+1, n+2\}$. Consider a bipartition $\mathcal{V}' = \mathcal{V}'_A \cup \mathcal{V}'_D$ such that $\mathcal{V}_A \subseteq \mathcal{V}'_A$ and $\mathcal{V}_D \subseteq \mathcal{V}'_D$, then the operation is called a 2-vertex addition if exactly three vertices among $i, j, n+1, n+2$ belong to $\mathcal{V}'_A$ and are non-collinear, and the fourth vertex belongs to $\mathcal{V}'_D$.

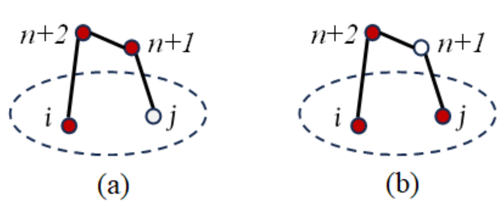

Fig. 5. 2-vertex additions. (a) The newly added two nodes belong to $\mathcal{V}_A$. (b) The newly added two nodes belong to $\mathcal{V}_D$. The dots in red represent nodes in $\mathcal{V}_A$.

Similarly, after performing a 2-vertex addition with vertices $n+1, n+2 \in \mathcal{V}'_A$, the induced framework $(\mathcal{G}'(A,D), p')$ is defined by

$$\mathcal{V}'_A \triangleq \mathcal{V}_A \cup \{n+1, n+2\}, \mathcal{V}'_D \triangleq \mathcal{V}_D,$$

$$\mathcal{E}' \triangleq \mathcal{E} \cup \{(j, n+1), (n+1, n+2), (n+2, i)\}, p' \triangleq [p^\top, p_{n+1}^\top, p_{n+2}^\top]^\top \in \mathbb{R}^{2(n+2)}.$$

Lemma 8. *Given a globally SA-RoD rigid framework $(\mathcal{G}(A,D), p)$ in $\mathbb{R}^2$, after performing a 2-vertex addition, the induced framework $(\mathcal{G}'(A,D), p')$ is globally SA-RoD rigid.*

Proof. Similar to the argument in Lemma 7, we only need to show the shape uniqueness of the quadrilateral $\Diamond ij, n+1, n+2$ under SA-RoD constraints provided in this lemma. One can also easily verify that $\Diamond ij, n+1, n+2$ is constrained by three SAs and one RoD. As long as three nodes in $\mathcal{V}_A$ are non-collinear, Proposition 2 indicates that the shape of the quadrilateral $\Diamond ij, n+1, n+2$ can be uniquely determined by SA-RoD constraints. $\square$

2.4.2 Construction of globally SA-RoD rigid frameworks

Based on vertex additions, we will construct some globally SA-RoD rigid frameworks in this subsection.

We begin by introducing a construction methodology, referred to as SA-RoD ordering, which is formally described in Algorithm 1. It can be observed that either a 1-vertex addition or a 2-vertex addition is performed at each step in Algorithm 1.

Algorithm 1 SA-RoD ordering for constructing $(\mathcal{G}_k(A,D), p(k))$

Start with $\mathcal{V} = \{1,2\}$, $p(2) = [p_1^\top, p_2^\top]^\top$, and $\mathcal{E} = \{(1,2)\}$.
while $|\mathcal{V}| < k$ **do**
  Perform a 1-vertex addition (including Type A_1, Type A_2, Type D_1, Type D_2)
  Or
  Perform a 2-vertex addition
end while

Next, we show how to construct minimally SA-RoD rigid frameworks. If a framework is constructed by an SA-RoD ordering consisting of k steps of 2-vertex additions, there exist $2k+2$ vertices and $3k+1$ edges. Additionally, if it can be constructed by k steps of 2-vertex additions and 1 step of 1-vertex addition, there exist $2k+1$ vertices and $3k$ edges. Thus, the lower bound in Lemma 6 is tight and frameworks constructed above are minimally SA-RoD rigid. Figure 6 shows an example of constructing minimally SA-RoD rigid frameworks.

Based on Lemma 7 and Lemma 8, the following theorem concerning global SA-RoD rigidity can be presented.

Theorem 9. *If a framework $(\mathcal{G}(A,D), p)$ is constructed by an SA-RoD ordering in $\mathbb{R}^2$, then it is globally SA-RoD rigid.*

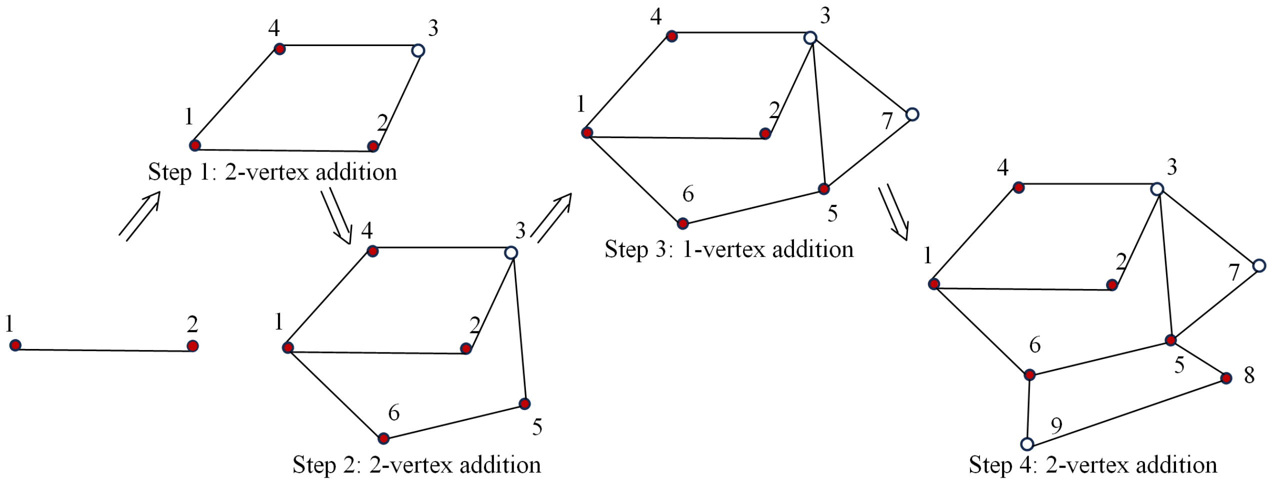

Fig. 6. Construction of minimally global SA-RoD rigid frameworks through vertex additions. The dots in red represent nodes in $\mathcal{V}_A$.

Now we introduce some special global SA-RoD rigid frameworks constructed by SA-RoD ordering. If a framework is purely constructed by 1-vertex additions in Algorithm 1, it is said to have a bilateration ordering [39]. Furthermore, if a bilateration ordering is generated by Type A_1 and Type D_1 1-vertex additions in turn, we call it a Type (A_1, D_1) bilateration ordering. Similarly, bilateration orderings of Type (D_1, A_1), Type (A_1, D_2), Type (A_2, D_1), Type (A_2, D_2), Type (D_2, A_1), Type (D_1, A_2), and Type (D_2, A_2) can be defined. If a framework is purely constructed by 2-vertex additions in Algorithm 1 and every edge lies in a quadrilateral, it is said to be a quadrilateralized framework.

Note that frameworks constructed by different SA-RoD orderings can exhibit different SA or RoD connectivity properties, which can affect localization algorithm synthesis to be discussed in Subsection 3.4. Specifically, in Algorithm 1, if 2-vertex additions and Type D_1 1-vertex additions occur in turn, we will obtain a framework, which is neither SA connected nor RoD connected. Such a framework is said to be generated by a Type $(2, D_1)$ SA-RoD ordering. For convenience, the detailed construction of a Type $(2, D_1)$ SA-RoD ordering is presented in Algorithm 2. Figure 7 presents three frameworks generated with a Type (D_1, A_1) bilateration ordering, 2-vertex additions and a Type $(2, D_1)$ SA-RoD ordering, respectively. Note that connectivity properties for these frameworks are completely different.

Algorithm 2 Type $(2, D_1)$ SA-RoD ordering for constructing $(\mathcal{G}_k(A, D), p(k))$

Start with $\mathcal{V} = \{1, 2\}$, $p(2) = [p_1^\top, p_2^\top]^\top$, and $\mathcal{E} = \{(1, 2)\}$. $\mathcal{V} \cap \mathcal{V}_A \neq \emptyset$, $\mathcal{V} \cap \mathcal{V}_D \neq \emptyset$.
while $|\mathcal{V}| < k - 1$ **do**
  Perform a 2-vertex addition
  if $|\mathcal{V}| < k$ **then**
    Perform a Type D_1 1-vertex addition
  end if
end while

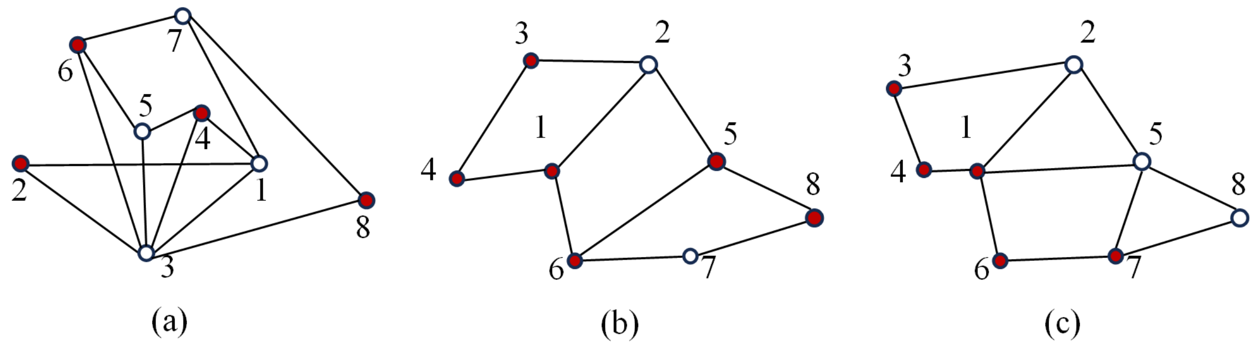

Fig. 7. (a) A framework with a Type (D_1, A_1) bilateration ordering. It is RoD connected over the underlying graph. (b) A quadrilateralized framework constructed by 2-vertex additions. It is SA connected over the underlying graph.(c) A framework with a Type $(2, D_1)$ SA-RoD ordering. It is neither RoD connected nor SA connected over the underlying graph. The dots in red represent nodes in $\mathcal{V}_A$.

2.4.3 Merging globally SA-RoD rigid frameworks

Merging is an important operation to maintain rigidity in formation control and network localization, which results in changes in the node set or interconnection structure of sensing and communication links. In this subsection, we study merging by two types of operations. The first type is connecting two globally SA-RoD rigid frameworks by adding edges. The second type is contracting vertices of two globally SA-RoD rigid frameworks. Existing works on merging distance or bearing rigid graphs can be found in [40] and [35].

Generally speaking, to ensure global bearing rigidity, three edges are required to be added in merging two existing smaller globally bearing rigid graphs in $\mathbb{R}^2$ [35]. We will show that under the setting of merging globally SA-RoD rigid frameworks, adding two edges suitably is sufficient to ensure global rigidity. The reason lies in the SA-RoD rigidity results of quadrilaterals in Proposition 2. We now state the following theorem. There might be a slight conceptual overlap $(A_i, D_i, i = 1, 2)$ in terms, but it will not cause any ambiguity.

Theorem 10 (Adding edges)**.** *Given two globally SA-RoD rigid frameworks* $(\mathcal{G}_1(A_1, D_1), p)$ *and* $(\mathcal{G}_2(A_2, D_2), q)$ *in* $\mathbb{R}^2$*, choose two vertices* $i, m \in \mathcal{V}_1$ *and* $j, k \in \mathcal{V}_2$ *and the merged framework* $(\mathcal{G}(A, D), r)$ *is denoted by* $\mathcal{V}_A = \mathcal{V}_{A_1} \cup \mathcal{V}_{A_2}, \mathcal{V}_D = \mathcal{V}_{D_1} \cup \mathcal{V}_{D_2}, r = [p^\top, q^\top]^\top$*, and* $\mathcal{E} = \mathcal{E}_1 \cup \mathcal{E}_2 \cup \{(m, k), (i, j)\}$*. If* $|\mathcal{V}_A \cap \{i, m, j, k\}| = 3$ *and corresponding three points are non-collinear, then* $(\mathcal{G}(A, D), r)$ *is globally SA-RoD rigid.*

The proof is presented in Appendix I. In fact, if the chosen four vertices i, m, j, k belong to $\mathcal{V}_A$ and corresponding four points are non-collinear, the newly merged framework by adding three edges is also globally SA-RoD rigid. The proof can be finished by a discussion of the shape uniqueness (combining Lemma 13 and Theorem 7).

So far, merging frameworks by adding edges has been considered. Analogously to Theorem 3.6 in [35], we present the second type of merging by contracting vertices of globally SA-RoD rigid frameworks in the following theorem. It is important to note that this type of operation is allowed only among vertices of the same attributes. The proof is similar to that of Theorem 10 and will be omitted.

Theorem 11 (Contracting vertices)**.** *Given two globally SA-RoD rigid frameworks* $(\mathcal{G}_1(A_1, D_1), p)$ *and* $(\mathcal{G}_2(A_2, D_2), q)$ *in* $\mathbb{R}^2$*, suppose there exist two vertex pairs* (i, j) *and* (m, k) *with* $i, m \in \mathcal{V}_1$ *and* $j, k \in \mathcal{V}_2$*, such that* $p_i = q_j, p_m = q_k$*, and vertices in each pair share the same attributes. Let* $\mathcal{V}_A = \mathcal{V}_{A_1} \cup \mathcal{V}_{A_2}, \mathcal{V}_D = \mathcal{V}_{D_1} \cup \mathcal{V}_{D_2}$*, and* $\mathcal{E} = \mathcal{E}_1 \cup \mathcal{E}_2$*. If the merged framework* $(\mathcal{G}(A, D), r)$ *is obtained from* $\mathcal{V}_A, \mathcal{V}_D, \mathcal{E}$ *and* $[p^\top, q^\top]^\top$ *by contracting vertex pairs* (i, j) *and* (m, k)*, then* $(\mathcal{G}(A, D), r)$ *is globally SA-RoD rigid.*

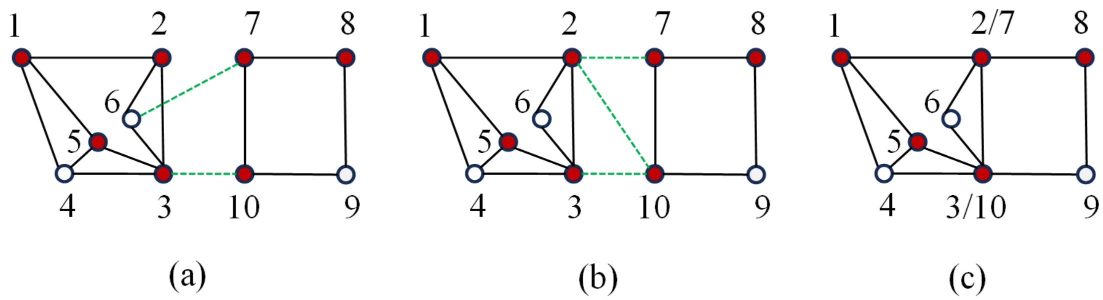

Fig. 8. Different merging approaches for two globally SA-RoD rigid frameworks. (a) Adding two edges $(6, 7)$ and $(3, 10)$. (b) Adding three edges $(2, 7), (2, 10)$ and $(3, 10)$. (c) Contracting vertices 7 and 2, vertices 10 and 3. The dots in red represent nodes in $\mathcal{V}_A$.

In Figure 8, two frameworks with vertices $\{1, 2, 3, 4, 5, 6\}$ and $\{7, 8, 9, 10\}$ are globally SA-RoD rigid. Three different merging approaches are presented by adding two edges, three edges and contracting vertices, respectively. If the four chosen vertices in Theorem 10 all belong to $\mathcal{V}_A$, adding three edges, such as $(2, 7), (2, 10)$ and $(3, 10)$ in Figure 8(b), can preserve the global SA-RoD rigidity when r_2, r_7, r_3, r_{10} are non-collinear. Similarly, contracting two pairs of vertices $(2, 7)$ and $(3, 10)$ as in Figure 8(c) can also ensure global SA-RoD rigidity.

3 SA-RoD-Based SNL

In this section, we will provide a mathematical formulation of the SA-RoD-based SNL problem. Then, we will discuss the localizability of sensor networks based on the developed rigidity theory. Furthermore, an edge-based localization approach will be proposed to determine the bearings and distances of edges in the underlying framework. After that, we will analyze the effects of SA/RoD connectivity on SNL and design localization algorithms.

3.1 Problem Formulation

Given a static sensor network in $\mathbb{R}^2$ composed of n_a anchors whose locations are known and n_f free nodes whose locations are to be determined. The sensor network is indexed by $\mathcal{V} = \mathcal{V}_a \cup \mathcal{V}_f$, where $\mathcal{V} = \{1, 2, \cdots, n\}, \mathcal{V}_a = \{1, 2, \cdots, n_a\}$ is the set of anchors, $\mathcal{V}_f = \{n_a + 1, n_a + 2, \cdots, n_a + n_f\}$ is the set of free nodes. Consider a connected undirected graph $\mathcal{G}(A,D)=(\mathcal{V}_A\cup\mathcal{V}_D,\mathcal{E})$ associated with a given bipartition of the vertex set representing the sensing graph among all nodes. Each sensor in $\mathcal{V}_A$ has the capability of measuring bearings of neighbor nodes in its local coordinate frame. That is, each sensor in $\mathcal{V}_A$ can sense SAs subtended at itself. Each sensor in $\mathcal{V}_D$ is capable of measuring RoDs with respect to any two neighbor nodes.

SNL in $\mathbb{R}^2$ aims at finding the locations of free nodes in $\mathcal{V}_f$ when locations of anchors in $\mathcal{V}_a$, SAs measured by sensors in $\mathcal{V}_A$, and RoDs measured by sensors $\mathcal{V}_D$ are provided. Figure 9 presents two sensor networks to illustrate SA-RoD-based SNL. Note that the only difference of two sensor networks lies in the type of measurements for sensor 6. In Figure 9(a), the position of sensors 3, 4, 5, 6 can be uniquely determined by the locations of anchors, measured SAs and RoDs. However, in Figure 9(b), the location of sensor 6 can not be uniquely determined due to a possible flipping ambiguity. This indicates the effects of bipartitions on SA-RoD-based SNL. Furthermore, note that the positions of sensors 4,5,6 can not be uniquely determined if the sensor network is purely constrained by SAs, while the positions of sensors 3,4,5,6 can not be uniquely determined if the sensor network is purely constrained by RoDs. This implies that neither the SA-based nor the RoD-based approach is applicable here.

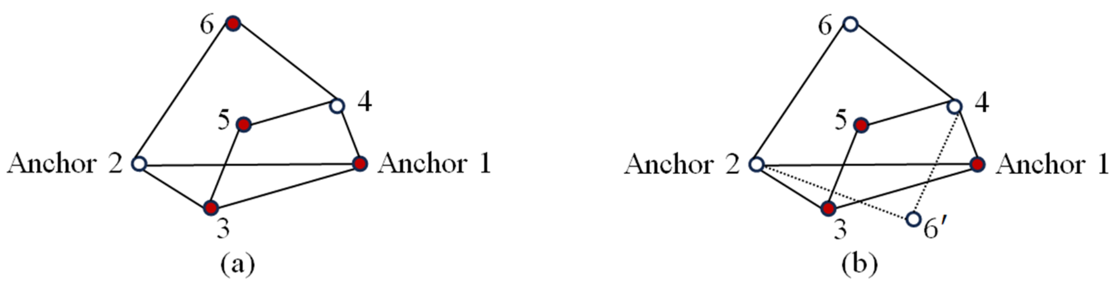

Fig. 9. (a) A sensor network where the locations of unknown sensors can be uniquely determined by positions of anchors, measured SAs and RoDs. (b) A sensor network where the locations of unknown sensors $3,4,5$ can be uniquely determined, but the location of sensor 6 can not be uniquely determined by positions of anchors, measured SAs and RoDs. Another possible location corresponds to $6'$. The dots in red represent nodes in $\mathcal{V}_A$.

Denote the location of sensor i as $x_i\in\mathbb{R}^2$, $x=[x_1^\top,\cdots,x_2^\top]^\top\in\mathbb{R}^{2n}$. The true locations of sensors are represented by $p=[p_1^\top,\cdots,p_n^\top]^\top\in\mathbb{R}^{2n}$. An important observation is that the bearing $\frac{x_i-x_j}{||x_i-x_j||}$ and distance $||x_i-x_j||$ can be obtained for any pair of anchors $i,j\in\mathcal{V}_a$ even if $(i,j)\notin\mathcal{E}$. Employing the handling in [13][21], the augmented framework $(\hat{\mathcal{G}}(A,D),x)$ is defined by $\hat{\mathcal{G}}=(\mathcal{V}_A\cup\mathcal{V}_D,\hat{\mathcal{E}})$ with $\hat{\mathcal{E}}=\mathcal{E}\cup\{(i,j)\in\mathcal{V}^2:i,j\in\mathcal{V}_a\}$. Namely, $\hat{\mathcal{E}}$ is obtained by adding edges to $\mathcal{E}$ which connect every pair of anchors to each other. In this paper, $(\hat{\mathcal{G}}(A,D),x,\mathcal{V}_a)$ represents a sensor network to be located and $(\hat{\mathcal{G}}(A,D),x)$ is called the underlying framework. Based on the aforementioned notions, the SA-RoD-based SNL problem can be formulated as follows.

Problem 1:

$$\text{find } x,$$

$$
\begin{aligned}
s.t.\ \frac{x_k - x_i}{||x_k - x_i||} &= \mathcal{R}(\theta_{ijk}) \frac{x_j - x_i}{||x_j - x_i||}, (i,j,k) \in \mathcal{T}_{\hat{A}}, \\
\frac{||x_t - x_r||}{||x_s - x_r||} &= \kappa_{rst}, (r,s,t) \in \mathcal{T}_{\hat{D}}, \\
x_i &= p_i, i \in \mathcal{V}_a,
\end{aligned} \tag{15}
$$

where $\kappa_{rst} = \frac{||p_t - p_r||}{||p_s - p_r||}$ is the RoD information measured by $r \in \mathcal{V}_D$, θ_{ijk} is the SA information measured by $i \in \mathcal{V}_A$, $\mathcal{T}_{\hat{A}} = \{(u,v,w) \in \mathcal{V}^3 : u \in \mathcal{V}_A, (u,v), (u,w) \in \hat{\mathcal{E}}, v < w\}$ is the SA index set determining all the SAs subtended in the framework, $\mathcal{T}_{\hat{D}} = \{(u,v,w) \in \mathcal{V}^3 : u \in \mathcal{V}_D, (u,v), (u,w) \in \hat{\mathcal{E}}, v < w\}$ is the RoD index set determining all the RoDs subtended in the framework.

To ensure that Problem 1 is meaningful, Assumption 3 is made in the following sections.

Assumption 3: Problem 1 is feasible, $\mathcal{V}_a \cap \mathcal{V}_A \neq \emptyset$, and $\mathcal{V}_a \cap \mathcal{V}_D \neq \emptyset$.

Note that the feasibility in Assumption 3 can always be satisfied for any sensor network if the measured SAs and RoDs are exact. The existence of both SA and RoD sensors in anchors can be guaranteed by manual settings in practice. All the results in the rest of the paper will be established under Assumption 3.

3.2 SA-RoD localizability

In this subsection, we will investigate whether the unknown nodes in a sensor network can be uniquely localized by locations of anchors, measured SAs and RoDs. First, we introduce the notion of SA-RoD localizability.

Definition 3.1. A sensor network is called SA-RoD localizable if there exists a unique feasible solution to (15).

If $n_a = 1$ and $q \in \mathbb{R}^{2n}$ is a solution to (15), an arbitraty rotation of q with anchor p_1 also gives a solution. Therefore, $n_a \geq 2$ for any SA-RoD localizable sensor network. Figures 10(a) and 10(b) present two sensor networks that are not SA-RoD localizable. One can also verify that the underlying frameworks are not globally SA-RoD rigid. The sensor network in Figure 10(c) is SA-RoD localizable and the underlying framework is globally SA-RoD rigid. We propose the following theorem to reveal the connection between SA-RoD localizability and global rigidity.

Theorem 12. *Under Assumption 3, a sensor network $(\hat{\mathcal{G}}(A,D), x, \mathcal{V}_a)$ is SA-RoD localizable if and only if the framework $(\hat{\mathcal{G}}(A,D), x)$ is globally SA-RoD rigid.*

The proof is presented in Appendix J. From the argument in the sufficient part, it can be observed that if $(\mathcal{G}(A,D), x)$ is globally SA-RoD rigid, $(\hat{\mathcal{G}}(A,D), x, \mathcal{V}_a)$ will be SA-RoD localizable as long as $n_a \geq 2$. This holds even when all anchors have the same sensing capabilities, thus relaxing the requirement of Assumption 3.

Corollary 2. *Suppose $(\mathcal{G}(A,D), x)$ is a globally SA-RoD rigid framework, if $n_a \geq 2$, then sensor network $(\hat{\mathcal{G}}(A,D), x, \mathcal{V}_a)$ is SA-RoD localizable.*

This corollary illustrates that for a globally SA-RoD rigid framework, an arbitrary choice of two anchors can ensure the localizability of the induced SN.

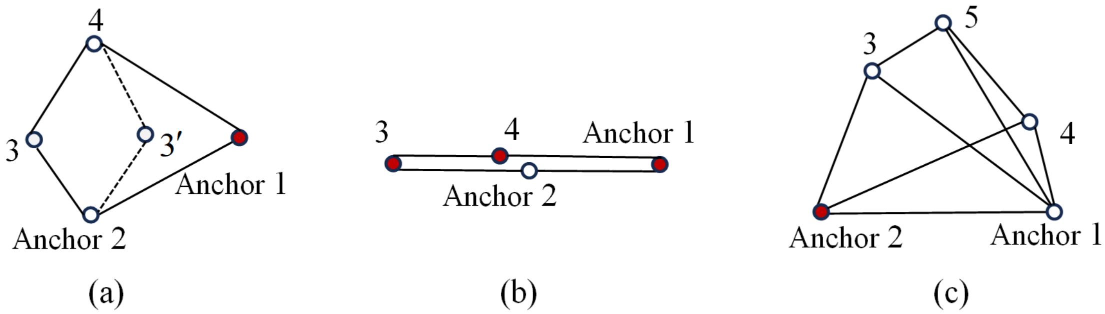

Fig. 10. (a) A sensor network that is not SA-RoD localizable. Node 3 may be incorrectly localized as 3′. However, if nodes 1 and 3 are anchors, this network becomes SA-RoD localizable. (b) A sensor network that is not SA-RoD localizable. Node 4 can move freely on the segment connecting nodes 1 and 3. (c) A sensor network that is SA-RoD localizable. The key point is that vertex 5 has degree 3 which avoids possible reflections. The dots in red represent nodes in $\mathcal{V}_A$.

3.3 An edge-based analysis

Based on the previous discussion, how to check the localizability of a sensor network (global SA-RoD rigidity of the corresponding framework) remains a difficult problem. In [41], a unified view on bearing-based localizability is proposed. The edge-based formulation of parallel rigidity was shown to be equivalent to the usual node-based formulation. In what follows, we also provide an edge-based approach in this subsection.

Definition 3.2. Let a graph cycle basis matrix of a graph $\mathcal{G}$ be expressed as $C = [c_{ij}] \in \mathbb{R}^{(m-n+1)\times m}$, where $c_{ij} \in \{\pm 1, 0\}$. Let $B = [\cdots, b_{ij}, \cdots] \in \mathbb{R}^{2\times m}$ be the bearing matrix of a framework $(\mathcal{G}, p)$, where $b_{ij} = \frac{p_i - p_j}{\|p_i - p_j\|}, (i,j) \in \mathcal{E}$. The cycle bearing matrix C_b for $(\mathcal{G}, p)$ is defined by $C_b = C \odot B \in \mathbb{R}^{2(m-n+1)\times m}$.

Denote the distances of all edges by $d = [d_1, \cdots, d_m]^\top \in \mathbb{R}^m_+$. Note that on each cycle $\mathcal{C}_k$, we have the following compatibility condition [41]:

$$\sum_{(i,j)\in\mathcal{E}} c_{k,ij} b_{ij} d_{ij} = 0, \;\; k = 1, 2\cdots, m-n+1, \tag{16}$$

where $c_{k,ij} = \pm 1$. Using the cycle bearing matrix, it can be written as:

$$C_b d = 0. \tag{17}$$

To solve SNL, we consider the following Problem 2 (an edge-based formulation).

Problem 2:

$$\begin{aligned} &\text{find } d_{ij}, \, b_{ij}, (i,j) \in \hat{\mathcal{E}} \\ &s.t. \;\; b_{ik} - \mathcal{R}(\theta_{ijk}) b_{ij} = 0, \;\; (i,j,k) \in \mathcal{T}_{\hat{A}}, \\ &\qquad d_{rt} - \kappa_{rst} d_{rs} = 0, \;\; (r,s,t) \in \mathcal{T}_{\hat{D}}, \end{aligned}$$

$$\sum_{(i,j)\in\mathcal{C}_k} c_{k,ij} d_{ij} b_{ij} = 0,\ k = 1,2,3,\cdots,m-n+1,$$
$$d_{ij} = d_{ij}^*,\ b_{ij} = b_{ij}^*,\ i,j \in \mathcal{V}_a,$$
$$d_{ij} > 0,\ ||b_{ij}|| = 1,\ (i,j) \in \hat{\mathcal{E}}. \tag{18}$$

Our next result reveals the intrinsic connection between Problem 1 and Problem 2. The proof is provided in Appendix K.

Theorem 13. *Under Assumption 3, Problem 1 is equivalent to Problem 2 given a fixed anchor position, in the sense that an explicit bijection can be built between the solution sets of these two problems.*

Without loss of generality, let $l \in \mathcal{V}_a$ be the base vertex of a path matrix P_l (see Definition K.1). According to Lemma 18, the explicit mapping to recover the solution of Problem 1 from that of Problem 2 is

$$x = \mathbf{1}_n \otimes x_l + P_l \odot Bd. \tag{19}$$

Comparing Problem 2 with Problem 1, we can find that the possible nonlinear constraints are caused by the compatibility constraint (17) and the unit norm of bearings $||b_{ij}|| = 1$ for $(i,j) \in \mathcal{E}$. All the other constraints in Problem 2 occur in linear forms, which will be very helpful for solving SNL in next section. Via Theorem 13, the following corollary about localizability can be derived.

Corollary 3. *Under Assumption 3, sensor network $(\hat{\mathcal{G}}(A,D), x, \mathcal{V}_a)$ is SA-RoD localizable if and only if there exists a unique solution to Problem 2.*

3.4 Solving SNL: the effects of SA/RoD connectivity

In this subsection, we aim to solve Problem 2. The analysis on structures of $\mathcal{T}_{\hat{A}}$ and $\mathcal{T}_{\hat{D}}$ will play a significant role. Interestingly, we will show that under some connectivity assumptions of $\mathcal{T}_{\hat{A}}$ and $\mathcal{T}_{\hat{D}}$, Problem 2 can be decoupled into two sub-problems of finding bearings and distances, respectively.

3.4.1 SNL with connected $\mathcal{T}_{\hat{A}}$ over $\hat{\mathcal{G}}$

As a consequence of Lemma 4, all the SAs corresponding to the total triple set $\mathcal{T}_{\hat{\mathcal{G}}}$ can be uniquely determined when the SA set $\mathcal{T}_{\hat{A}}$ is connected over $\hat{\mathcal{G}}$. By solving Sub-problem 1, all bearings of edges can be derived.

Sub-problem 1:

$$\begin{cases} b_{ik} - \mathcal{R}(\theta_{ijk}) b_{ij} = 0,\ (i,j,k) \in \mathcal{T}_{\hat{A}}, \\ b_{ij} = b_{ij}^*,\ i,j \in \mathcal{V}_a. \end{cases} \tag{20}$$

Then, we propose Sub-problem 2 to find distances of all edges in the original framework.

Sub-problem 2:

$$\begin{cases} d_{ik} - \kappa_{ijk} d_{ij} = 0, \ (i,j,k) \in \mathcal{T}_{\hat{D}}, \\ \displaystyle\sum_{(i,j)\in\mathcal{C}_k} c_{k,ij} b_{ij} d_{ij} = 0, \ k = 1,2,3,\cdots, m-n+1, \\ d_{ij} = d^*_{ij}, \ i,j \in \mathcal{V}_a. \end{cases} \tag{21}$$

Denote $s = |\mathcal{T}_{\hat{D}}| + \frac{n_a(n_a-1)}{2} + 2(m-n+1)$. In addition, $D_0 \in \mathbb{R}^{[|\mathcal{T}_D| + \frac{n_a(n_a-1)}{2}]\times m}$ is defined as

$$\begin{array}{c} \\ \cdots \\ \kappa_{ijk} \\ \cdots \\ d_{st} \\ \cdots \end{array} \begin{array}{c} \begin{array}{ccccccc} \cdots & \text{edge } (i,j) & \cdots & \text{edge } (i,k) & \cdots & \text{edge } (s,t) & \cdots \end{array} \\ \begin{pmatrix} \cdots & \cdots & \cdots & \cdots & \cdots & \cdots & \cdots \\ \mathbf{0} & -\kappa_{ijk} & \mathbf{0} & 1 & \mathbf{0} & 0 & \mathbf{0} \\ \cdots & \cdots & \cdots & \cdots & \cdots & \cdots & \cdots \\ \mathbf{0} & 0 & \mathbf{0} & 0 & \mathbf{0} & 1 & \mathbf{0} \\ \cdots & \cdots & \cdots & \cdots & \cdots & \cdots & \cdots \end{pmatrix} \end{array}, \tag{22}$$

where the rows are indexed by triplets in $\mathcal{T}_{\hat{D}}$ and distances among anchors. If we denote $C_D = [C_b^\top, D_0^\top]^\top \in \mathbb{R}^{s\times m}$, $y = [0,\cdots,0,d^*_{ij},\cdots]^\top \in \mathbb{R}^s$, where C_b is the cycle bearing matrix, then Equation (21) can be compactly written as

$$C_D d = y. \tag{23}$$

Now we can state the following theorem.

Theorem 14. *Under Assumption 3, if $\mathcal{T}_{\hat{A}}$ is connected over $\hat{\mathcal{G}}$, then sensor network $(\hat{\mathcal{G}}(A,D), x, \mathcal{V}_a)$ is localizable if and only if* $\text{rank}(C_D) = m$.

Proof. Since $\mathcal{T}_{\hat{A}}$ is connected over $\hat{\mathcal{G}}$, all bearings of edges can be uniquely determined by (20). From Corollary 3, $(\hat{\mathcal{G}}(A,D), x, \mathcal{V}_a)$ is localizable if and only if there exists a unique solution to Problem 2. Equivalently, there exists a unique solution to (23). Based on Assumption 3, there exists a feasible solution to (23). Therefore, the uniqueness of the solution to (23) is equivalent to $\text{rank}(C_D) = m$. $\square$

For Problem 2, bearings and distances can be determined by solving (20) and (23), respectively. In addition to a concise criterion of the SA-RoD localizability, this theorem also provides a practical localization approach by solving linear equations. More precisely, we summarize this approach in Algorithm 3.

Algorithm 3 SNL with connected $\mathcal{T}_{\hat{A}}$ over $\hat{\mathcal{G}}$

Find bearings of all edges by solving (20)
Find distances of all edges by solving (23)
Reconstruct locations of unknown sensors based on (19)

3.4.2 SNL with connected $\mathcal{T}_{\hat{D}}$ over $\hat{\mathcal{G}}$

Similarly, if $\mathcal{T}_{\hat{D}}$ is connected over $\hat{\mathcal{G}}$, distances of all edges can be uniquely determined by solving Sub-problem 3.

Sub-problem 3:

$$\begin{cases} d_{ik} - \kappa_{ijk} d_{ij} = 0, \ (i,j,k) \in \mathcal{T}_{\hat{D}}, \\ d_{ij} = d_{ij}^*, \ i,j \in \mathcal{V}_a. \end{cases} \tag{24}$$

Then, finding bearings of all edges can be achieved by solving Sub-problem 4.

Sub-problem 4:

$$\begin{cases} \sum_{(i,j)\in\mathcal{C}_k} c_{k,ij} b_{ij} d_{ij} = 0, \ k = 1,2,3,\cdots, m-n+1, \\ b_{ik} - \mathcal{R}(\theta_{ijk}) b_{ij} = 0, \ (i,j,k) \in \mathcal{T}_{\hat{A}}, \\ b_{ij} = b_{ij}^*, \ i,j \in \mathcal{V}_a, \\ ||b_{ij}|| = 1, \ (i,j) \in \hat{\mathcal{E}}. \end{cases} \tag{25}$$

Denote $C_{B,1} = (C \odot [\cdots, d_{ij}, \cdots]) \otimes I_2$, $t = 2(m-n+1) + 2|\mathcal{T}_{\hat{A}}| + n_a(n_a - 1)$, $C_B = [C_{B,1}^\top, C_{B,2}^\top]^\top \in \mathbb{R}^{t\times 2m}$, $b = [\cdots, b_{ij}^\top, \cdots]^\top \in \mathbb{R}^{2m}$, $z = [0, \cdots, 0, \cdots, b_{ij}^{*\top}, \cdots]^\top \in \mathbb{R}^t$, where $C_{B,2}$ is defined by

$$\begin{array}{c} \\ \cdots \\ \theta_{ijk} \\ \cdots \\ b_{st} \\ \cdots \end{array} \begin{array}{c} \begin{array}{ccccccc} \cdots & \text{edge } (i,j) & \cdots & \text{edge } (i,k) & \cdots & \text{edge } (s,t) & \cdots \end{array} \\ \begin{pmatrix} \cdots & \cdots & \cdots & \cdots & \cdots & \cdots & \cdots \\ \mathbf{0} & -\mathcal{R}(\theta_{ijk}) & \mathbf{0} & I_2 & \mathbf{0} & 0_{2\times 2} & \mathbf{0} \\ \cdots & \cdots & \cdots & \cdots & \cdots & \cdots & \cdots \\ \mathbf{0} & 0_{2\times 2} & \mathbf{0} & 0_{2\times 2} & \mathbf{0} & I_2 & \mathbf{0} \\ \cdots & \cdots & \cdots & \cdots & \cdots & \cdots & \cdots \end{pmatrix} \end{array}, \tag{26}$$

where the rows are indexed by triplets in $\mathcal{T}_{\hat{A}}$ and bearings among anchors. Thus, a compact form of (25) is

$$\begin{cases} C_B b = z, \\ ||b(2k-1:2k)|| = 1, \ k = 1,2,\cdots, m. \end{cases} \tag{27}$$

From Assumption 3, we know that there exists at least one solution to (25). First, using Penrose-Moore inverse, all solutions of $C_B b = z$ can be represented as

$$b = C_B^\dagger z + [\tilde{b}_1, \cdots, \tilde{b}_L] w = C_B^\dagger z + \sum_{i=1}^{L} w_i \tilde{b}_i, \tag{28}$$

where $L = \dim(\text{null}(C_B))$, $\text{null}(C_B) = \text{span}\{\tilde{b}_i\}_{i=1}^L$, and $w = [w_1, w_2, \cdots, w_L]^\top \in \mathbb{R}^L$ is the variable to be solved. Let $N_B = [\tilde{b}_1, \cdots, \tilde{b}_L] \in \mathbb{R}^{m\times L}$, then (28) can be rewritten as

$$b = C_B^\dagger z + N_B w. \tag{29}$$

Denote $E_k = \text{diag}(\mathbf{0}, 1, 1, \mathbf{0}) \in \mathbb{R}^{2m\times 2m}$, where 1 occurs at the $2k-1$-th and $2k$-th locations. So the norm constraints $||b(2k-1:2k)|| = 1$ can be expressed as

$$(C_B^\dagger z + N_B w)^\top E_k (C_B^\dagger z + N_B w) = 1, \ k = 1,2,\cdots, m. \tag{30}$$

Denote $H(w) = \sum_{k=1}^{m} [(C_B^{\dagger} z + N_B w)^{\top} E_k (C_B^{\dagger} z + N_B w) - 1]^2$, (30) can be equivalently transformed into:

$$H(w) = 0, \ w \in \mathbb{R}^L. \tag{31}$$

Despite the difficulty caused by the non-convexity of $H(\cdot)$, this problem has been greatly simplified to an equation on the null space. Such optimization problems have been extensively investigated by various approaches, such as interior point methods, sequential quadratic methods, etc. Analogously to the argument in Theorem 14, we present the following theorem. The proof is omitted here.

Theorem 15. *Under Assumption 3, if $\mathcal{T}_{\hat{D}}$ is connected over $\hat{\mathcal{G}}$, then sensor network $(\hat{\mathcal{G}}(A, D), x, \mathcal{V}_a)$ is localizable if and only if* (31) *has a unique solution.*

This theorem illustrates the equivalence between localizability and the uniqueness of global minimizers of $H(\cdot)$ on $\mathbb{R}^L$ when $\mathcal{T}_D$ is connected over $\mathcal{G}$. For Problem 2, bearings and distances are determined by solving (24) and (31). More precisely, we summarize this localization approach into Algorithm 4.

Algorithm 4 SNL with connected $\mathcal{T}_{\hat{D}}$ over $\hat{\mathcal{G}}$

Find distances of all edges by solving (24)
Find bearings of all edges by solving (29) and (31)
Reconstruct locations of unknown sensors based on (19)

We note that solving (31) or verifying the uniqueness of global minimizers of $H(\cdot)$ remains a time-consuming task. Fortunately, for some special frameworks such as frameworks constructed by Type (D_1, A_1) bilaterion orderings (see Figure 7(a)), a concise description of null(C_B) can be derived to remove the quadratic constraints $||b(2k-1:2k)|| = 1$ in (27). We will show that under this setting, the matrix $C_B \in \mathbb{R}^{t \times (4n-6)}$ is of full column rank.

Proposition 3. *Under Assumption 3, suppose that $(\hat{\mathcal{G}}(A, D), x)$ is generated by a Type (D_1, A_1) bilateration ordering and $\mathcal{V}_a = \{1, 2\}$, then* rank$(C_B) = 4n - 6$ *for sensor network $(\hat{\mathcal{G}}(A, D), x, \mathcal{V}_a)$.*

The proof of Proposition 3 is given in Appendix L. As a consequence, we have null$(C_B) = 0$. Now we present the following theorem without proof.

Theorem 16. *Under Assumption 3, suppose that $(\hat{\mathcal{G}}(A, D), x)$ is generated by a Type (D_1, A_1) bilateration ordering and $\mathcal{V}_a = \{1, 2\}$, then the bearing vector satisfies $b = C_B^{\dagger} z$ for sensor network $(\hat{\mathcal{G}}(A, D), x, \mathcal{V}_a)$.*

3.4.3 SNL with disconnected $\mathcal{T}_{\hat{A}}$ and $\mathcal{T}_{\hat{D}}$ over $\hat{\mathcal{G}}$

In this part, we discuss SNL in the setting that neither $\mathcal{T}_{\hat{D}}$ nor $\mathcal{T}_{\hat{A}}$ is connected over $\hat{\mathcal{G}}$. Suppose that the triple index graphs of $\mathcal{T}_{\hat{A}}$ and $\mathcal{T}_{\hat{D}}$ have c_A, c_D connected components, respectively. It can be shown that the localization problem can be reduced to solving a polynomial equation with $2c_A + c_D - 3$ variables. To state related results, the following lemma is essential.

Lemma 9. *The solution spaces V_A and V_D of* (20) *and* (24) *are affine with dimensions* $2(c_A - 1)$ *and* $c_D - 1$*, respectively.*

The proof is presented in Appendix M. Based on this lemma, solution spaces V_A and V_D can be parameterized as follows.

$$
\begin{aligned}
V_A &= \{b = \tilde{b}_0 + \sum_{i=1}^{2c_A-2} w_i \tilde{b}_i : w_i \in \mathbb{R}, i = 1, 2, \cdots, 2c_A - 2\}, \\
V_D &= \{d = \tilde{d}_0 + \sum_{i=1}^{c_D-1} y_j \tilde{d}_j : y_j \in \mathbb{R}, j = 1, 2, \cdots, c_D - 1\}.
\end{aligned} \tag{32}
$$

Denote $\tilde{V}_A = \text{span}\{\tilde{b}_i : i = 1, 2, \cdots, 2c_A - 2\}$, $\tilde{V}_D = \text{span}\{\tilde{d}_i : i = 1, 2, \cdots, c_D - 1\}$. In order to solve the localization problem, we need to investigate the remained constraints of the cycle condition and unit norm of bearing vectors:

$$
\begin{cases} C_{B,1} b = 0, \\ ||b(2k-1:2k)|| = 1, \ k = 1, 2, \cdots, m. \end{cases} \tag{33}
$$

It should be noted that under previous parameterizations, the first constraint is generally nonlinear with quadratic terms since $C_{B,1}$ also contains undetermined variables. Similarly, let $G(w, y) = ||C_{B,1} b||^2 + \sum_{i=1}^{m} [b^\top E_i b - 1]^2$, where b, d are parameterized by $w \in \mathbb{R}^{2c_A-2}, y \in \mathbb{R}^{c_D-1}$ as in (32). Therefore, (33) can be equivalently expressed in a concise form as

$$
G(w, y) = 0, \tag{34}
$$

along with the following constraint

$$
\tilde{d}_0 + \sum_{i=1}^{c_D-1} y_j \tilde{d}_j > 0 \tag{35}
$$

on $\mathbb{R}^{2c_A-2} \times \mathbb{R}^{c_D-1}$. Similarly, we can present the following algebraic characterization of localizable sensor networks when both SA constraints and RoD constraints are disconnected.

Theorem 17. *Under Assumption 3, sensor network* $(\hat{\mathcal{G}}(A, D), x, \mathcal{V}_a)$ *is localizable if and only if there exists a unique solution to* (34) *and* (35)*.*

For the edge-based localization problem, bearing vectors and distances are determined by solving two sub-problems (20), (24) and (34). The theorem above actually provides a solution method based on dimension reduction. Solving (34) satisfying (35) can be achieved through classical optimization methods, which have been discussed in textbooks such as [42]. Similarly, the localization approach is presented in Algorithm 5.

Algorithm 5 SNL with disconnected $\mathcal{T}_{\hat{A}}$ and $\mathcal{T}_{\hat{D}}$ over $\hat{\mathcal{G}}$

Find w, y by solving (34) and (35)
Find bearings and distances of all edges by (32)
Reconstruct locations of unknown sensors based on (19)

4 Numerical simulations

In this section, we provide some numerical examples to validate the efficacy of the proposed SNL method. The nodes of sensor networks in all examples are supposed to lie in the unit box $[0,1]^2$ randomly. Furthermore, the number of nodes is 70 and there exist 2 anchors in each network. All simulations are executed using Matlab R2024b with an Intel® Core™ i9-13900 CPU and 33.6 GB RAM.

Example 1: Figure 11(a) shows a quadrilateralized sensor network generated via 2-vertex additions, which has 103 edges and is SA connected over the underlying graph. Computational results indicate that $\mathrm{rank}(C_D) = 103$. Based on Algorithm 3, the estimated positions of all nodes can be recovered as illustrated in Figure 11(b). It is obvious that these estimated locations match the true locations of nodes closely. Here the mean squared error between the estimated locations and true locations can be calculated to be $8.1398e{-}15$. In addition, the computation time is 0.0845s.

In contrast, Figure 11(c) presents a quadrilateralized sensor network that is SA connected, but not constructed by 2-vertex additions. Although this network also has 103 edges, the rank of C_D in this case is 101, which is less than the total number of edges. According to Theorem 14, this sensor network is not localizable. In Figure 11(d), we can find some incorrectly localized nodes (marked with red asterisks). This is consistent with the conclusion in Theorem 14.

Example 2: The sensor network in Figure 12(a) is generated by a Type (D_1, A_1) bilateration ordering, which is RoD connected over the underlying graph. Based on the fact that the underlying graph is a Laman graph, the number of edges is $m = 2n - 3 = 137$. First, after a computation, we find that $\mathrm{rank}(C_B) = 4n - 6 = 274$ and derive a unique solution to (24), which is consistent with Proposition 3. Then we recover the locations of unknown sensors using Algorithm 4. This process only involves linear equation solvers. As shown in Figure 12(b), the estimated locations also match the true locations of nodes closely. In this case, the computation time is 0.1373s and the mean squared error is $7.2709e - 14$.

Example 3: Figure 12(c) presents a sensor network which has 169 edges and is RoD connected over the underlying graph. The underlying framework is built iteratively from an initial quadrilateral through a sequence of Type D_2 and Type A_1 1-vertex additions. Similarly, one can solve (24) and verify that $\mathrm{rank}(C_B) = 334$ and the codimension of C_B is $2m - \mathrm{rank}(C_B) = 4$. Hence, (31) is a nonlinear polynomial equation with 4 variables. Based on Algorithm 4, the locations of unknown sensors can be estimated as shown in Figure 12(d). We can observe that the estimated locations also match the true locations of nodes closely. In this case, the computation time is 0.7323s and the mean squared error is $4.6063e - 04$.

Example 4: The sensor network in Figure 12(e) is generated by a Type $(2, D_1)$ SA-RoD ordering, which has 114 edges. According to the construction, there exist 23 connected components in $\mathcal{T}_{\hat{A}}$ and 47 connected components in $\mathcal{T}_{\hat{D}}$. A numerical calculation provides $\dim(V_A) = 44$ and $\dim(V_D) = 46$. This is consistent with Lemma 9. Hence, (31) is a nonlinear polynomial equation with 90 variables. As shown in Figure 12(f), we can also obtain the estimated locations close to the true locations of nodes by Algorithm 5. In this example, the computation time is 1.7187s and the mean squared error is $6.8477e - 06$.

5 Conclusions and future directions

This work established the SA-RoD rigidity theory for frameworks with bipartitions on the vertex sets. It has been shown that a duality theorem holds for infinitesimally SA-RoD rigid frameworks with respect to bipartitions. Furthermore, if $\mathcal{T}_A$ or $\mathcal{T}_D$ is connected over the underlying graph $\mathcal{G}$, the framework $(\mathcal{G}(A, D), p)$ can inherit the SA or RoD rigidity property of $(\mathcal{G}, p)$. Additionally, the shapes of frameworks constructed by SA-RoD orderings can be uniquely determined by SA and RoD constraints. The SA-RoD rigidity theory was employed in the SNL problem with heterogeneous nodes. The SA-RoD-based SNL was investigated from the perspective of an edge-based approach. Our results indicated that the connectivity of $\mathcal{T}_{\hat{A}}$ or $\mathcal{T}_{\hat{D}}$ over $\hat{\mathcal{G}}$ can help to decouple the SNL problem into two sub-problems of solving distances and bearings successively. When both $\mathcal{T}_{\hat{A}}$ and $\mathcal{T}_{\hat{D}}$ are disconnected, a parameterization method was proposed to effectively reduce the dimension of the solution space.

Meaningful future work may include: 1) searching a partition for the vertex set of a graph to minimize the number of edges associated with a configuration such that the framework is (globally) rigid, 2) extending the proposed rigidity theory to frameworks in $\mathbb{R}^3$ (the SA constraints may be replaced with unsigned angle constraints), 3) investigating SNL by optimization methods under noisy measurements, 4) developing distributed localization protocols for SNL.

6 Appendix

A Preliminaries

In this section, we will briefly review some mathematical tools in algebraic graph theory and important results in distance/RoD and bearing/SA rigidity theory.

A.1 Algebraic graph theory

Given a graph $\mathcal{G} = (\mathcal{V}, \mathcal{E})$, a path of length l from vertices i to j is a sequence of $l+1$ distinct adjacent vertices starting with i and ending with j. A cycle $\mathcal{C}$ represents a path with the same starting and ending vertices. In other words, a cycle is a connected subgraph, where each vertex has exactly two neighbor vertices. A graph with no cycles is called acyclic. A tree refers to a connected acyclic graph. A spanning tree is an acyclic spanning subgraph.

Definition A.1 (Oriented graph[43]). An orientation of a graph $\mathcal{G}$ is the assignment of a direction to each edge. Equivalently, it is a function σ of all arcs such that if (i, j) is an arc, then $\sigma(i, j) = -\sigma(j, i)$.

And a graph together with a specific orientation is called an oriented graph.

Definition A.2 (Cut space and flow space[43])**.** For an oriented graph G, the cut space is a subspace of $\mathbb{R}^m$ corresponding the column space of the incidence matrix H. And the flow space is the orthogonal complement of the cut space.

For a cycle $\mathcal{C}_l$ of length l in the oriented graph $\mathcal{G}$, one can define the oriented cycle with a signed characteristic vector $z \in \mathbb{R}^l$ as

$$z_e \triangleq \begin{cases} 1 & e \text{ is consistent with the orientation,} \\ -1 & e \text{ is opposite to the orientation,} \\ 0 & e \text{ is not in the cycle } \mathcal{C}. \end{cases} \tag{36}$$

Lemma 10 (Dimension and Base of flow space[43])**.** *Given a connected graph $\mathcal{G}$ with n vertices and m edges, its flow space has dimension $m - n + 1$. Furthermore, this space is spanned by the signed characteristic vectors of its cycles.*

It should be noted that the flow space is also called the cycle space and these independent cycles can be obtained by adding chords to a maximal spanning tree of $\mathcal{G}$. A matrix with rows corresponding to $m - n + 1$ independent signed characteristic vectors of cycles is called a cycle basis matrix.

A.2 Graph rigidity theory

For a graph $\mathcal{G}$, if every vertex i is assigned with a coordinate $p_i \in \mathbb{R}^d$, then $p = [p_1^\top, p_2^\top, \cdots, p_n^\top]^\top \in \mathbb{R}^{nd}$ is called a configuration of graph $\mathcal{G}$, and $(\mathcal{G}, p)$ is called a framework. A configuration $p \in \mathbb{R}^{nd}$ is said to be non-degenerate if $p_1, p_2, \cdots, p_n$ do not lie on a common hyperplane of $\mathbb{R}^d$, and $(\mathcal{G}, p)$ is called a non-degenerate framework.

In different types of rigidity theory, the rigidity function $f_\mathcal{G} : \mathbb{R}^{nd} \to \mathbb{R}^q$ is first defined. For example, the distance rigidity function is

$$f_\mathcal{G}(p) \triangleq [\cdots, ||p_i - p_j||^2, \cdots]^\top, \ (i, j) \in \mathcal{E}. \tag{37}$$

We say a framework $(\mathcal{G}, p)$ is rigid if $f_\mathcal{G}^{-1}(f_\mathcal{G}(p)) \cap U_p = f_\mathcal{K}^{-1}(f_\mathcal{K}(p)) \cap U_p$ for some neighborhood $U_p \subseteq \mathbb{R}^{nd}$ of p. If $f_\mathcal{G}^{-1}(f_\mathcal{G}(p)) = f_\mathcal{K}^{-1}(f_\mathcal{K}(p))$, $(\mathcal{G}, p)$ is said to be globally rigid. $(\mathcal{G}, p)$ is minimally rigid in $\mathbb{R}^d$ if and only if there does not exist any subgraph $\mathcal{H}$ with n vertices and less than m edges such that $(\mathcal{H}, p)$ is rigid in $\mathbb{R}^d$. Due to the nonlinear behaviors of rigidity functions, we usually expand them to the first order near a specific framework to define infinitesimal rigidity. The Jacobi matrix $R_\mathcal{G}(p) = \frac{\partial f_\mathcal{G}}{\partial p}$ is called the rigidity matrix. Vectors in the kernel of $R_\mathcal{G}(p)$ are called infinitesimal motions, which ensure the invariance of the rigidity function $f_\mathcal{G}$. If the rigidity function is defined by RoDs (bearings, SAs), similar notions can also be proposed in RoD (bearing, SA) rigidity theory. Here we briefly review some results useful for later discussion.

A.2.1 Distance rigidity theory versus RoD rigidity theory

In RoD rigidity theory, the rigidity function can be defined as

$$f_{\mathcal{G}}(p) \triangleq [\cdots, \frac{||p_i - p_k||^l}{||p_i - p_j||^l}, \cdots]^\top, \ (i,j,k) \in \mathcal{T}_{\mathcal{G}}, l \in \mathbb{Z}^+, \tag{38}$$

where $\mathcal{T}_{\mathcal{G}} = \{(i,j,k) : (i,j),(i,k) \in \mathcal{E}, j < k\}$.

Lemma 11 (Relations between RoD rigidity and distance rigidity theory[16])**.** *(Infinitesimal/Global) RoD rigidity of a framework is equivalent to its (infinitesimal/global) distance rigidity.*

A.2.2 Bearing rigidity theory versus SA rigidity theory

In bearing rigidity theory, the rigidity function is defined as

$$f_{\mathcal{G}}(p) \triangleq [\cdots, b_{ij}^\top, \cdots]^\top, \ (i,j) \in \mathcal{E}, \tag{39}$$

where $b_{ij}(p) = \frac{p_j - p_i}{||p_j - p_i||}$. The infinitesimal bearing rigidity of a framework implies its bearing rigidity. Bearing rigidity of a framework is equivalent to its global bearing rigidity[12].

In SA rigidity theory[14] [15], the rigidity function is defined as

$$f_{\mathcal{G}}(p) \triangleq [\cdots, \alpha_{ijk}, \cdots]^\top, \ (i,j,k) \in \mathcal{T}_{\mathcal{G}}, \tag{40}$$

where $\alpha_{ijk} \in [0, 2\pi)$ can be uniquely determined by

$$\alpha_{ijk} = \begin{cases} \text{acos}(b_{ij}^\top b_{ik}), & b_{ik}^\top \mathcal{R}(\pi/2) b_{ij} \geq 0, \\ 2\pi\text{-acos}(b_{ij}^\top b_{ik}), & b_{ik}^\top \mathcal{R}(\pi/2) b_{ij} < 0. \end{cases} \tag{41}$$

Lemma 12 (Relations between SA rigidity and bearing rigidity theory[15])**.** *(Infinitesimal/Global) SA rigidity of a framework in $\mathbb{R}^2$ is equivalent to its (infinitesimal/global) bearing rigidity.*

Lemma 13 (Shape determination by SAs[15])**.** *Given a framework $(\mathcal{G}, p)$ in $\mathbb{R}^2$, the following statements are equivalent:*
(i) $(\mathcal{G}, p)$ is infinitesimally SA rigid;
(ii) $(\mathcal{G}, p)$ is non-degenerate and globally SA rigid;
(iii) The shape of $(\mathcal{G}, p)$ can be uniquely determined by SAs up to uniform rotations, translations, and scalings.

A.2.3 Generic property

A configuration p is said to be generic if the coordinates of p do not satisfy any non-zero polynomial equations with integer coefficients, and $(\mathcal{G}, p)$ is called a generic framework. It is well-known that generic configurations are dense in the space of all configurations. The set of all non-generic frameworks is of measure zero[44]. In distance rigidity theory, Laman graphs are perhaps the most well-known due to their beautiful properties and simple construction process.

Definition A.3. Graph $\mathcal{G} = (\mathcal{V}, \mathcal{E})$ is called a Laman graph if $m = 2n - 3$ and there exist less than $2k - 3$ edges for every subgraph of $\mathcal{G}$ with $k \geq 2$ vertices.

An equivalent characterization is that a Laman graph can always be obtained by the Henneberg constructions[44]. Henneberg constructions include two types of operations: vertex addition and edge splitting.

For distance/bearing/SA constrained frameworks, underlying graphs are discovered to play a key role in constructing (global) rigid frameworks. Specifically, infinitesimal distance/bearing/SA rigidity is a generic property of the underlying graph. In other words, for a given graph $\mathcal{G}$, suppose that there exists one generic configuration $p \in \mathbb{R}^{nd}$ such that $(\mathcal{G}, p)$ is infinitesimally distance/bearing/SA rigid. Then for any generic configuration $q \in \mathbb{R}^{nd}$, $(\mathcal{G}, q)$ is infinitesimally distance/bearing/SA rigid [44, 12, 15]. In distance rigidity theory, the following Laman's Theorem is well-known.

Lemma 14 (Laman's theorem[44])**.** *In $\mathbb{R}^2$, a graph is generically minimally distance rigid if and only if it is a Laman graph.*

In [45], the authors show that Laman graphs are generically bearing rigid. More interestingly, in $\mathbb{R}^2$, the generic bearing rigidity of a graph is equivalent to the existence of a Laman spanning subgraph.

B Proof of Lemma 1

Proof. Denote

$$D_{ij} = \frac{b_{ij}}{||e_{ij}||},\ D_{ik} = \frac{b_{ik}}{||e_{ik}||},\ D_{ijk} = D_{ij} - D_{ik},$$
$$A_{ij} = \mathcal{R}(\pi/2) D_{ij},\ A_{ik} = \mathcal{R}(\pi/2) D_{ik}\, A_{ijk} = A_{ij} - A_{ik}.$$

Therefore, the SA-RoD rigidity matrix $R_{\mathcal{G}_{A,D}}(p)$ can be expressed in the following form:

$$\begin{array}{c} \\ \cdots \\ \alpha_{rst} \\ \cdots \\ \kappa_{ijk} \\ \cdots \end{array}
\begin{array}{c}
\begin{array}{cccccccc} \cdots & \text{vertex } i & \text{vertex } r & \text{vertex } j & \text{vertex } s & \text{vertex } k & \text{vertex } t & \cdots \end{array} \\
\begin{pmatrix}
\cdots & \cdots & \cdots & \cdots & \cdots & \cdots & \cdots & \cdots \\
\mathbf{0} & 0_{1\times 2} & A_{rst}^\top & 0_{1\times 2} & -A_{rs}^\top & 0_{1\times 2} & A_{rt}^\top & \mathbf{0} \\
\cdots & \cdots & \cdots & \cdots & \cdots & \cdots & \cdots & \cdots \\
\mathbf{0} & \kappa_{ijk} D_{ijk}^\top & 0_{1\times 2} & -\kappa_{ijk} D_{ij}^\top & 0_{1\times 2} & \kappa_{ijk} D_{ik}^\top & 0_{1\times 2} & \mathbf{0} \\
\cdots & \cdots & \cdots & \cdots & \cdots & \cdots & \cdots & \cdots
\end{pmatrix}
\end{array}, \tag{42}$$

where the rows are indexed by the triplet sets $\mathcal{T}_D$ and $\mathcal{T}_A$, the columns are indexed by the vertices.

We consider the linear dependence relations of the row vectors in $R_{\mathcal{G}(A,D)}$. If $i \in \mathcal{V}_D$, let $j_0 = \text{argmin}_{j \in \mathcal{N}_i} j$. After fixing the edge $(i, j_0) \in \mathcal{E}$, consider the triplets at node i formed by this edge with all other $\deg(i) - 1$ edges. It holds that $\kappa_{ij_0j_1} \kappa_{ij_1j_2} = \kappa_{ij_0j_2}$ whenever $j_0 < j_1 < j_2 \in \mathcal{N}_i$. The partial diffrential regarding p can be obtained as

$$\frac{\partial \kappa_{ij_1j_2}}{\partial p} = \kappa_{ij_0j_1}^{-1} [\frac{\partial \kappa_{ij_0j_2}}{\partial p} - \kappa_{ij_1j_2} \frac{\partial \kappa_{ij_0j_1}}{\partial p}].$$

So the vector $\frac{\partial \kappa_{ij_1j_2}}{\partial p}$ can be expressed as a linear combination of vectors $\frac{\partial \kappa_{ij_0j_1}}{\partial p}$ and $\frac{\partial \kappa_{ij_0j_2}}{\partial p}$. Similarly, all the vectors in the set $\{\frac{\partial \kappa_{ijk}}{\partial p} : j < k \in \mathcal{N}_i\}$ can be written as linear combinations of vectors in the set $\{\frac{\partial \kappa_{ij_0k}}{\partial p} : k \in \mathcal{N}_i, k \neq j_0\}$. Note that the cardinality of the latter set is $\deg(i) - 1$. Then,

$$\dim(\mathrm{span}\{\frac{\partial \kappa_{ijk}}{\partial p} : j < k \in \mathcal{N}_i\}) \leq \deg(i) - 1.$$

A more direct argument shows that this conclusion also holds if $i \in \mathcal{V}_A$. In other words, the rank of sub-matrix corresponding to constraints at node i in (42) is less than $\deg(i) - 1$. Using

$$\mathrm{rank}[X^\top, Y^\top]^\top \leq \mathrm{rank}(X) + \mathrm{rank}(Y)$$

(X,Y are two matrices of suitable size) inductively, we can derive that

$$\mathrm{rank}(R_{\mathcal{G}_{A,D}}(p)) \leq \sum_{i \in \mathcal{V}} [\deg(i) - 1] = 2|\mathcal{E}| - |\mathcal{V}| = 2m - n.$$

Thus, the proof is finished. $\square$

C Proof of Lemma 2

Whenever it does not cause ambiguity, the bipartition in this proof is omitted in writting graph $\mathcal{G}$ or $\mathcal{K}$ instead of $\mathcal{G}(A, D)$ or $\mathcal{K}(A, D)$ for the sake of brevity.

Proof. Suppose that $f_{\mathcal{K}}(q) = f_{\mathcal{K}}(p)$ for some $q \in \mathbb{R}^{2n}$. Assume $i \in \mathcal{V}_A, j \in \mathcal{V}_D$, let $c = \frac{||q_i - q_j||}{||p_i - p_j||}$ and $\theta \in [0, 2\pi)$ be the signed angle rotating from the direction of $p_i - p_j$ to that of $q_i - q_j$. Thus,

$$q_i - q_j = c\mathcal{R}(\theta)(p_i - p_j). \tag{43}$$

Let $\xi = q_i - c\mathcal{R}(\theta)p_i$, it can be easily verified that

$$q_k = \xi + c\mathcal{R}(\theta)p_k, k = i, j. \tag{44}$$

Our goal is to show that

$$q_k = \xi + c\mathcal{R}(\theta)p_k, k \neq i, j. \tag{45}$$

Case 1: $k \in \mathcal{V}_A$. Consider the triangle Δijk (may be degenerate), two signed angles spanned at node $\alpha_{ijk}, \alpha_{kij}$ are known, then the third signed angle can also be determined by $\alpha_{jik} = \pi + \alpha_{ijk} + \alpha_{kij} \mod 2\pi$. If the triangle Δijk is non-degenerate, then RoDs can be uniquely determined by the standard sine law. If the triangle Δijk is degenerate, that is i, j, k are collinear. Without loss of generality, assume $\alpha_{ijk} = \alpha_{kij} = 0, \alpha_{jik} = \pi$, utilizing the RoD $\kappa_{jik} = ||p_k - p_j||/||p_i - p_j||$, we can obtain that $\kappa_{ijk} = 1 + \kappa_{jik}, \kappa_{kij} = \kappa_{jik}/(1 + \kappa_{jik})$. Therefore, all the RoDs and SAs in the triangle

Δijk are determined. Thus, using (43), it follows that

$$\begin{aligned} q_i - q_k &= \frac{||q_i - q_k||}{||q_i - q_j||}\mathcal{R}(\alpha_{ijk})(q_i - q_j) = c\frac{||q_i - q_k||}{||q_i - q_j||}\mathcal{R}(\alpha_{ijk})\mathcal{R}(\theta)(p_i - p_j) \\ &= c\mathcal{R}(\theta)\frac{||p_i - p_k||}{||p_i - p_j||}\mathcal{R}(\alpha_{ijk})(p_i - p_j) = c\mathcal{R}(\theta)(p_i - p_k). \end{aligned} \tag{46}$$

Using (44), one can directly derive (45).

Case 2: $k \in \mathcal{V}_D$. There are two nodes measuring RoDs in the triangle $\Delta p_i p_j p_k$. Similarly, all the RoDs and SA α_{ijk} are determined. One can show that all the SAs can be determined no matter whether the triangle is degenerate or not. Following a similar routine in case 1, one can finish the proof. □

D Proof of Lemma 3

Proof. According to the definition of S_p, we construct a mapping as follows:

$$F : [0, 2\pi) \times \mathbb{R}^2 \times \mathbb{R}^+ \to S_p \subseteq \mathbb{R}^{2n},$$

$$F(\theta, \xi, c) \triangleq \mathbf{1}_n \otimes \xi + c(I_n \otimes \mathcal{R}(\theta))p.$$

Step 1: We will show that F is a bijective mapping. The definition of S_p indicates that F is surjective. To show its injectivity, suppose $F(\theta, \xi, c) = F(\theta', \xi', c')$, that is,

$$\mathbf{1}_n \otimes \xi + c(I_n \otimes \mathcal{R}(\theta))p = \mathbf{1}_n \otimes \xi' + c'(I_n \otimes \mathcal{R}(\theta'))p.$$

In component form, this is equivalent to

$$\xi + c\mathcal{R}(\theta)p_i = \xi' + c'\mathcal{R}(\theta')p_i, i = 1, 2, \cdots, n. \tag{47}$$

For $i \neq j$, we obtain

$$c\mathcal{R}(\theta)(p_i - p_j) = c'\mathcal{R}(\theta')(p_i - p_j). \tag{48}$$

Since $p_i \neq p_j$ when $i \neq j$, analyzing the norms on both hand sides of (48) provides that $c = c' > 0$ and $\theta = \theta' \in [0, 2\pi)$. Substituting these into (47), we can conclude that $\xi = \xi'$.

Step 2: We will show that S_p is a 4-dimensional smooth manifold. First, we show that for each $q \in S_p$, there exists a neighborhood $U_q \subseteq S_p$ that is homeomorphic to an open set $U \subseteq \mathbb{R}^4$. If $q \in S_p$, there exist prameters $\theta_0 \in [0, 2\pi), \xi_0 \in \mathbb{R}^2, c_0 > 0$ such that $q = F(\theta_0, \xi_0, c_0) = \mathbf{1}_n \otimes \xi_0 + c_0(I_n \otimes \mathcal{R}(\theta_0))p$.

If $\theta_0 \neq 0$, let $\delta = \min\{|\theta_0|, |\theta_0 - 2\pi|\}$, $U_q = \{q' = \mathbf{1}_n \otimes \xi + c(I_n \otimes \mathcal{R}(\theta))p : \theta \in (\theta_0 - \delta, \theta_0 + \delta), \xi \in \mathbb{R}^2, c \in (0, +\infty)\}$. One can observe that $(\theta_0 - \delta, \theta_0 + \delta) \subseteq [0, 2\pi)$ and $U_q \subseteq S_p$ is a neighborhood near q. Based on results in step 1, $F : (\theta_0 - \delta, \theta_0 + \delta) \times \mathbb{R}^2 \times \mathbb{R}^+ \to U_q$ is bijective. One can also verify its inverse mapping is also continuous. So U_q is homeomorphic to the open set $(\theta_0 - \delta, \theta_0 + \delta) \times \mathbb{R}^2 \times \mathbb{R}^+ \subseteq \mathbb{R}^4$.

If $\theta_0 = 0$, we take $U_q = \{q' = \mathbf{1}_n \otimes \xi + c(I_n \otimes \mathcal{R}(\theta))p : \theta \in (-\pi, \pi), \xi \in \mathbb{R}^2, c \in (0, +\infty)\}$. Although $(-\pi, \pi)$ is not included in $[0, 2\pi)$, using the periodicity of the rotation matrix $\mathcal{R}(\theta)$ and arguments in step 1 also shows that $F : (-\pi, \pi) \times \mathbb{R}^2 \times \mathbb{R}^+ \to U_q$ is a homeomorphism.

Therefore, S_p is a 4-dimensional topological manifold. The transition map in different charts can be verified to be smooth. Therefore, S_p is a 4-dimensional smooth manifold.

Step 3: We will show that F is a smooth immersion into $\mathbb{R}^{2n}$. The smoothness of mapping F is obvious. To verify the immersion, we calculate the rank of its Jacobi map. The i-th block of the Jacobi matrix $DF \in \mathbb{R}^{2n\times 4}$ is $[I_2, c\frac{d}{d\theta}\mathcal{R}(\theta)p_i, \mathcal{R}(\theta)p_i] = [I_2, c\mathcal{R}(\theta+\frac{\pi}{2})p_i, \mathcal{R}(\theta)p_i]$, where we have applied the identity $\frac{d}{d\theta}\mathcal{R}(\theta) = \mathcal{R}(\theta+\frac{\pi}{2})$. Denote the four columns as

$$v_1 = [1, 0, 1, 0, \cdots, 1, 0]^\top, v_2 = [0, 1, 0, 1, \cdots, 0, 1]^\top,$$

$$v_3 = c[(\mathcal{R}(\theta+\pi/2)p_1)^\top, \cdots, (\mathcal{R}(\theta+\pi/2)p_n)^\top]^\top, v_4 = [(\mathcal{R}(\theta)p_1)^\top, \cdots, (\mathcal{R}(\theta)p_n)^\top]^\top.$$

Assume there exist some coefficients $c_i \in \mathbb{R}, i = 1, 2, 3, 4$ such that $c_1v_1 + c_2v_2 + c_3v_3 + c_4v_4 = 0$. Denote $e_1 = [1, 0]^\top, e_2 = [0, 1]^\top$. In component form, we have

$$c_1e_1 + c_2e_2 + c_3c\mathcal{R}(\theta+\pi/2)p_i + c_4\mathcal{R}(\theta)p_i = 0, i = 1, 2\cdots, n. \tag{49}$$

Similarly as in 48, we have

$$c_3c\mathcal{R}(\theta+\pi/2)(p_i - p_j) + c_4\mathcal{R}(\theta)(p_i - p_j) = 0, i \neq j. \tag{50}$$

Since $\mathcal{R}(\theta+\pi/2)(p_i - p_j)$ is orthogonal to $\mathcal{R}(\theta)(p_i - p_j)$, it is natural that $c_3 = c_4 = 0$. Combining with (49), $c_1 = c_2 = 0$. Thus, $\text{rank}(DF_p) = 4$. Therefore, F is a smooth immersion.

Consider the well-known parameterization of the unit circle $\mathbb{S}^1$ by an exponential mapping $E : [0, 2\pi) \to \mathbb{S}^1$ $(E(t) = \exp(\sqrt{-1}t))$. Define $\tilde{F} : \mathbb{S}^1 \times \mathbb{R}^2 \times \mathbb{R}^+ \to S_p \subseteq \mathbb{R}^{2n}$,

$$\tilde{F}(z, \xi, c) = F(E^{-1}(z), \xi, c) = \mathbf{1}_n \otimes \xi + c(I_n \otimes \mathcal{R}(E^{-1}(z)))p.$$

Combining step 1 and step 2, $\tilde{F}$ is bijective and of rank 4. Based on the global constant rank theorem (Theorem 4.14 in reference [46]), $\tilde{F}$ is a diffeomorphism. $\square$

E Proof of Theorem 6

Proof. We only need to show that

$$\dim(\text{null}(R_{\mathcal{G}(A,D)}(p))) = \dim(\text{null}(R_{\mathcal{G}'(A,D)}(p))).$$

Based on the expression (42), suppose $x = [x_1^\top, \cdots, x_n^\top]^\top \in \text{null}(R_{\mathcal{G}(A,D)}(p))$. Then,

$$D_{ijk}^\top x_i - D_{ij}^\top x_j + D_{ik}^\top x_k = 0,\ (i, j, k) \in \mathcal{T}_D,$$

$$A_{rst}^\top x_r - A_{rs}^\top x_s + A_{rt}^\top x_t = 0,\ (r, s, t) \in \mathcal{T}_A.$$

Using the orthogonal relations between $D.$ and $A.$, we have

$$A_{ijk}^{\top}\mathcal{R}(\pi/2)x_i - A_{ij}^{\top}\mathcal{R}(\pi/2)x_j + A_{ik}^{\top}\mathcal{R}(\pi/2)x_k = 0,\ (i,j,k) \in \mathcal{T}_D = \mathcal{T}_A',$$

$$D_{rst}^{\top}\mathcal{R}(\pi/2)x_r - D_{rs}^{\top}\mathcal{R}(\pi/2)x_s + D_{rt}^{\top}\mathcal{R}(\pi/2)x_t = 0,\ (r,s,t) \in \mathcal{T}_A = \mathcal{T}_D'.$$

That is $(I_n \otimes \mathcal{R}(\pi/2))x \in \mathrm{null}(R_{\mathcal{G}'(A,D)}(p))$. Therefore, we can construct a linear mapping F : $\mathrm{null}(R_{\mathcal{G}(A,D)}(p)) \to \mathrm{null}(R_{\mathcal{G}'(A,D)}(p))$ as follows: $F(x) = (I_n \otimes \mathcal{R}(\pi/2))x$. Furthermore, it is easy to verify that F is injective. Thus,

$$\dim(\mathrm{null}(R_{\mathcal{G}(A,D)}(p))) \leq \dim(\mathrm{null}(R_{\mathcal{G}'(A,D)}(p))).$$

Similarly, $\dim(\mathrm{null}(R_{\mathcal{G}'(A,D)}(p))) \leq \dim(\mathrm{null}(R_{\mathcal{G}(A,D)}(p)))$. Thus, we have finished the proof. □

F Proof of Proposition 2

Proof. Case 1: $\mathcal{V}_A = \{1\}$, $\mathcal{V}_D = \{2,3,4\}$. The shape of triangle $\Delta 124$ can be uniquely determined by α_{124} and $\kappa_{213}\kappa_{324}\kappa_{413}^{-1} = \frac{d_{14}}{d_{12}}$. Furthermore, the shape of triangle $\Delta 234$ can also be uniquely determined by RoDs in this triangle. To ensure the shape uniqueness of $\Diamond 1234$, the possible reflection of node 3 with respect to the line connecting nodes 2 and 4 should be avoided. This is equivalent to that nodes $2,3,4$ are collinear or the reflection of node 3 with respect to the line connecting nodes 2 and 4 leads to the same location as node 1, i.e., $d_{14} = d_{34}, d_{12} = d_{32}$.

Case 2: $\mathcal{V}_A = \{1,2\}$, $\mathcal{V}_D = \{3,4\}$. Equation (11) can be rewritten as

$$\begin{bmatrix} \cos\theta_{12} & \frac{d_{34}}{d_{14}} & 0 \\ \sin\theta_{12} & 0 & \frac{d_{34}}{d_{14}} \end{bmatrix} \begin{bmatrix} \frac{d_{12}}{d_{14}} \\ \cos\theta_{34} \\ \sin\theta_{34} \end{bmatrix} = -\begin{bmatrix} \cos\theta_{23} & \cos\theta_{41} \\ \sin\theta_{23} & \sin\theta_{41} \end{bmatrix} \begin{bmatrix} \frac{d_{23}}{d_{14}} \\ 1 \end{bmatrix}. \tag{51}$$

Denote

$$M_1 = \begin{bmatrix} \cos\theta_{12} & \frac{d_{34}}{d_{14}} & 0 \\ \sin\theta_{12} & 0 & \frac{d_{34}}{d_{14}} \end{bmatrix}, y = -\begin{bmatrix} \cos\theta_{23} & \cos\theta_{41} \\ \sin\theta_{23} & \sin\theta_{41} \end{bmatrix} \begin{bmatrix} \frac{d_{23}}{d_{14}} \\ 1 \end{bmatrix}.$$

We investigate solutions of the following equation:

$$M_1 x = y \tag{52}$$

Since p always corresponds to a feasible solution, $[\frac{d_{12}}{d_{14}}, \cos\theta_{34}, \sin\theta_{34}]^{\top}$ is a solution of (52). Furthermore, we have $\mathrm{null}(M) = \mathrm{span}\{[1, -\frac{d_{14}}{d_{34}}\cos\theta_{12}, -\frac{d_{14}}{d_{34}}\sin\theta_{12}]^{\top}\}$. Thus, the solution set of (52) is

$$\{[\frac{d_{12}}{d_{14}}, \cos\theta_{34}, \sin\theta_{34}]^{\top} + t[1, -\frac{d_{14}}{d_{34}}\cos\theta_{12}, -\frac{d_{14}}{d_{34}}\sin\theta_{12}]^{\top} : \frac{d_{12}}{d_{14}} + t > 0, t \in \mathbb{R}\}.$$

Considering the unit norm constraints of bearing vectors, we have

$$||[\cos\theta_{34} - t\frac{d_{14}}{d_{34}}\cos\theta_{12}, \sin\theta_{34} - t\frac{d_{14}}{d_{34}}\sin\theta_{12}]|| = 1.$$

Solving this equation gives $t = 0$ or $t = 2\frac{d_{34}}{d_{14}}\cos(\theta_{34} - \theta_{12})$. If $\frac{d_{12}}{d_{14}} + 2\frac{d_{34}}{d_{14}}\cos(\theta_{34} - \theta_{12}) > 0$, there exist two feasible RoDs subtended at node 1. From Theorem 7, $(\mathcal{G}(A, D), p)$ is not globally SA-RoD rigid. If $\frac{d_{12}}{d_{14}} + 2\frac{d_{34}}{d_{14}}\cos(\theta_{34} - \theta_{12}) \leq 0$, there exists a unique feasible RoD subtended at node 1. Utilizing geometrical constraints in triangles $\Delta 124$ and $\Delta 234$, all RoDs and SAs can be uniquely determined. Therefore, it is globally SA-RoD rigid if and only if

$$d_{12} + 2d_{34}\cos(\theta_{34} - \theta_{12}) \leq 0. \tag{53}$$

An example which is not globally SA-RoD rigid and violates (53) is presented in Figure 1(d).
Case 3: $\mathcal{V}_A = \{1, 3\}$, $\mathcal{V}_D = \{2, 4\}$. Invoking the cosine law in triangles $\Delta 234$ and $\Delta 124$, one has

$$d_{23}^2 + d_{34}^2 - 2d_{23}d_{34}\cos\theta_{324} = d_{12}^2 + d_{14}^2 - 2d_{12}d_{14}\cos\theta_{124}.$$

Combining with RoD constraints, we can conclude that the variable $x = \frac{d_{14}}{d_{12}} > 0$ satisfies

$$(1 - \kappa_{413}^2)x^2 - 2(\cos\theta_{124} - \kappa_{413}\kappa_{213}\cos\theta_{324})x + 1 - \kappa_{213}^2 = 0.$$

Then a direct geometrical observation provides that the shape of a quadrilateral is uniquely determined if and only if this equation has a unique positive solution. Note that for a given framework, this equation always has a feasible positive solution. If $\kappa_{413} = 1$, i.e., $d_{14} = d_{34}$, this equation degenerates into a linear equation. Consequently, the uniqueness of positive solutions is guaranteed. Otherwise, $d_{14} \neq d_{34}$. Under this setting, to ensure a unique positive solution, there exist two possibilities:
(a) There exist two equal positive roots. Consequently, the discriminant of this quadratic equation is 0, i.e.,

$$\kappa_{413}^2 + \kappa_{213}^2 - \sin^2\theta_{124} - \kappa_{413}^2\kappa_{213}^2\sin^2\theta_{324} - 2\kappa_{413}\kappa_{213}\cos\theta_{324}\cos\theta_{124} = 0.$$

Thus, we have

$$d_{12}^2d_{34}^2 + d_{14}^2d_{23}^2 - d_{14}^2d_{21}^2\sin^2\theta_{124} - d_{34}^2d_{23}^2\sin^2\theta_{324} - 2d_{12}d_{23}d_{34}d_{14}\cos\theta_{324}\cos\theta_{124} = 0. \tag{54}$$

(b) There exist two distinct roots. Furthermore, one root is positive while the other is non-positive. We have

$$x_1x_2 = \frac{1 - \kappa_{213}^2}{1 - \kappa_{413}^2} \leq 0.$$

Equivalently, it can be derived that

$$(d_{23} - d_{12})(d_{34} - d_{14}) \leq 0. \tag{55}$$

Note that the possibility of $d_{34} = d_{14}$ is also included in this inequality. Figure 1(e) shows a framework that is not globally SA-RoD rigid and violates (13), (14).
Case 4: Three nodes measure SAs and the fourth one measures RoDs, i.e., $\mathcal{V}_A = \{1, 2, 3\}$, $\mathcal{V}_D = \{4\}$.

All SAs and $\frac{d_{13}}{d_{14}}$ can be obtained. Equation (11) can be equivalently written as

$$\begin{bmatrix} \cos\theta_{12} & \cos\theta_{23} \\ \sin\theta_{12} & \sin\theta_{23} \end{bmatrix} \begin{bmatrix} \frac{d_{12}}{d_{14}} \\ \frac{d_{23}}{d_{14}} \end{bmatrix} = -\begin{bmatrix} \cos\theta_{34} & \cos\theta_{41} \\ \sin\theta_{34} & \sin\theta_{41} \end{bmatrix} \begin{bmatrix} \frac{d_{34}}{d_{14}} \\ 1 \end{bmatrix}. \tag{56}$$

Denote

$$M_2 = \begin{bmatrix} \cos\theta_{12} & \cos\theta_{23} \\ \sin\theta_{12} & \sin\theta_{23} \end{bmatrix}, \ z = -\begin{bmatrix} \cos\theta_{34} & \cos\theta_{41} \\ \sin\theta_{34} & \sin\theta_{41} \end{bmatrix} \begin{bmatrix} \frac{d_{34}}{d_{14}} \\ 1 \end{bmatrix}.$$

We investigate solutions of the following equation:

$$M_2 x = z. \tag{57}$$

Similarly, $[\frac{d_{12}}{d_{14}}, \frac{d_{23}}{d_{14}}]^\top$ is always a feasible solution to (57). Note that $\det(M_2) = \sin(\theta_{23} - \theta_{12})$. So there exists a unique solution to (57) if and only if $\sin(\theta_{23} - \theta_{12}) \neq 0$, i.e., nodes 1, 2 and 3 are non-collinear. From Theorem 7, $(\mathcal{G}(A, D), p)$ is globally SA-RoD rigid if and only if nodes 1, 2 and 3 are non-collinear. $\square$

G Proof of Theorem 8

Before presenting the proof, we recall that for q is said to be a regular point of a smooth mapping $h : \mathbb{R}^k \to \mathbb{R}^l$ if $\text{rank}(\frac{\partial h}{\partial p}(q)) = \max_{p\in\mathbb{R}^k} \text{rank}(\frac{\partial h}{\partial p}(p))$. Then, we provide the following Lemma.

Lemma 15. *Given a graph $\mathcal{G}(A, D)$ with an arbitrary bipartition, if $p \in \mathbb{R}^{2n}$ is generic, then p is a regular point of $f_{\mathcal{G}(A,D)}$.*

Proof. Assume $k = \max_{p\in\mathbb{R}^{2n}} \text{rank}(\frac{\partial f_{\mathcal{G}(A,D)}}{\partial p}(p)) = \max_{p\in\mathbb{R}^{2n}} \text{rank}(R_{\mathcal{G}(A,D)}(p))$, then there exists a square k-by-m minor of $R_{\mathcal{G}(A,D)}(p)$ whose rank is k. We denote the determinant of this minor as $h(p)$, which is a non-zero function. Suppose that q is not a regular point of $f_{\mathcal{G}(A,D)}$, i.e., $\text{rank}(R_{\mathcal{G}(A,D)}(q)) < k$. Thus, we have $h(q) = 0$. We denote the set of edges involved in this particular minor as $\mathcal{E}_1$.

Recalling the expression of the rigidity matrix $R_{\mathcal{G}(A,D)}$ in (42), the elements are in the form of $\frac{b_{ij}}{||e_{ij}||} = \frac{p_j - p_i}{||p_j - p_i||^2}$(a rational function of the coordinates), $\kappa_{ijk}\frac{b_{ij}}{||e_{ij}||} = ||p_k - p_i||\frac{p_j - p_i}{||p_j - p_i||^3} = ||p_k - p_i||||p_j - p_i||\frac{p_j - p_i}{||p_j - p_i||^4}$(a product of a rational function and square root functions). Following the routine in section IV of reference [20], the space $\mathbb{L}(\mathcal{E}_1)$ can be defined as

$$\mathbb{L}(\mathcal{E}_1) = \left\{ \sum_{F\in 2^{\mathcal{E}_1}} P_F(x_1, x_2, \cdots, x_n) \prod_{(i,j)\in F} d_{x_i,x_j} : P_F \in \mathbb{Q}(x_1, x_2, \cdots, x_n) \right\}, \tag{58}$$

where $2^{\mathcal{E}_1}$ is the power set of $\mathcal{E}_1$, $\mathbb{Q}(x_1, x_2, \cdots, x_n)$ is the field of rational functions with rational coefficients, $d_{x_i,x_j} = ||x_i - x_j||$. Let $|\mathcal{E}_1| = m_1$. According to Lemma 3 in [20], $\mathbb{L}(\mathcal{E}_1)/\mathbb{Q}(x_1, x_2, \cdots, x_n)$ is a field extension of degree 2^{m_1}. Furthermore, $h \in \mathbb{L}(\mathcal{E}_1)$. Since $q \in \mathbb{R}^{2n}$ is generic satisfying $h(q) = 0$, Lemma 4 in [20] illustrates that $h = 0$. Thus, we have obtained a contradiction to the fact that h is a non-zero function. $\square$

Then, we will show that for generic frameworks, SA-RoD rigidity and infinitesimal SA-RoD rigidity are equivalent.

Lemma 16. *Given a graph $\mathcal{G}(A, D)$ with an arbitrary bipartition and a generic configuration $p \in \mathbb{R}^{2n}$, then framework $(\mathcal{G}(A, D), p)$ is SA-RoD rigid if and only if it is infinitesimally SA-RoD rigid.*

Proof. Necessarity: Since $(\mathcal{G}(A, D), p)$ is SA-RoD rigid with a generic configuration p. Based on Lemma 15, p is a regular point of $f_{\mathcal{G}(A,D)}$. Let $\text{rank}(R_{\mathcal{G}(A,D)}(p)) = k$. According to Proposition 2 in [36] , there exists a neighborhood U of p such that $f^{-1}_{\mathcal{G}(A,D)}(f_{\mathcal{G}(A,D)}(p)) \cap U$ is a $2n - k$ dimensional manifold. Based on Lemma 2 and Lemma 3, SA-RoD rigidity of $(\mathcal{G}(A, D), p)$ implies that $2n - k = 4$. Thus, $k = 2n - 4$, i.e., $(\mathcal{G}(A, D), p)$ is infinitesimally SA-RoD rigid.

Sufficiency: It is a consequence of Theorem 2. □

Proof of Theorem 8. Based on Lemma 16, we only need to show the result for infinitesimal SA-RoD rigidity. Suppose that $p^* \in \mathbb{R}^{2n}$ is generic, $(\mathcal{G}(A, D), p^*)$ is infinitesimally SA-RoD rigid. So $\text{rank}(R_{\mathcal{G}(A,D)}(p^*)) = \max_{p \in \mathbb{R}^{2n}} \text{rank}(R_{\mathcal{G}(A,D)}(p)) = 2n - 4$. Let $q \in \mathbb{R}^{2n}$ be a generic point distinct to p^*. Based on Lemma 15, we have $\text{rank}(R_{\mathcal{G}(A,D)}(q)) = \max_{p \in \mathbb{R}^{2n}} \text{rank}(R_{\mathcal{G}(A,D)}(p)) = 2n-4$. Therefore, $(\mathcal{G}(A, D), q)$ is infinitesimally SA-RoD rigid. □

H Proof of Lemma 7

Proof. For a Type A_1 1-vertex addition, without loss of generality, assume $i, n+1 \in \mathcal{V}'_A, j \in \mathcal{V}'_D$. From the global SA-RoD rigidity of the framework $(\mathcal{G}(A, D), p)$, there exist at least two neighbors of node i and node j. Assume $(m, i) \in \mathcal{E},\ (l, j) \in \mathcal{E},\ m \neq j,\ l \neq i$. Based on Theorem 7, the SA α_{jli} and RoD α_{imj} can be uniquely determined by SA and RoD constraints no matter whether $(i, j) \in \mathcal{E}$. Since $i \in \mathcal{V}'_A, j \in \mathcal{V}'_A$, the SA $\alpha_{jl,n+1}$ and RoD $\kappa_{im,n+1}$ are constrained. By algebraic properties of SAs and RoDs, we have

$$\kappa_{ij,n+1} = \kappa_{im,n+1}/\kappa_{imj}, \alpha_{ji,n+1} = \alpha_{jl,n+1} - \alpha_{jli}.$$

In addition, the SA $\alpha_{ji,n+1}$ is constrained. In consequence, there exist constraints of two SAs and one RoD in the triangle $\Delta ij, n+1$(may be degenerate). Thus, the shape of the triangle $\Delta ij, n+1$ is uniquely determined and no reflection of node $n+1$ can occur. So $(\mathcal{G}'(A, D), p')$ is globally SA-RoD rigid.

Then, we briefly sketch the proof for other types. For a Type A_2 1-vertex addition, we have $i, j, n+1 \in \mathcal{V}'_A$. If these three points are non-collinear, the shape uniqueness of $\Delta ij, n+1$ under SA constraints can be guaranteed. A similar argument can provide global SA-RoD rigidity of the induced framework. For a Type D_1 1-vertex addition, the proof can be conducted similarly. For a Type D_2 1-vertex addition, we have $i, j, k, n+1 \in \mathcal{V}'_D$. Similarly, we know $\kappa_{ik,n+1}, \kappa_{ij,n+1}, \kappa_{kj,n+1}$ can be uniquely determined by SA and RoD constraints. Combining with RoDs $\kappa_{n+1,i,k}$ and $\kappa_{n+1,i,j}$, the shapes of triangle $\Delta ik, n+1$ and triangle $\Delta jk, n+1$ can be uniquely determined. Since points i, j, k are non-collinear, the flipping ambiguity of point $n+1$ is circumvented. So the induced framework is globally SA-RoD rigid. □

I Proof of Theorem 10

Proof. Without loss of generality, assume $i \in \mathcal{V}_D, m, j, k \in \mathcal{V}_A$. For simplicity, we use $f_{\mathcal{G}}$ to represent the rigidity function $f_{\mathcal{G}(A,D)}$. To show $f_{\mathcal{G}}^{-1}(f_{\mathcal{G}}(p)) = S_r$, it is sufficient to prove $f_{\mathcal{G}}^{-1}(f_{\mathcal{G}}(r)) \subseteq S_r$. Let $r' = [p'^T, q'^T]^\top \in f_{\mathcal{G}}^{-1}(f_{\mathcal{G}}(r))$, then we have $f_{\mathcal{G}_1}(p') = f_{\mathcal{G}_1}(p)$ and $f_{\mathcal{G}_2}(q') = f_{\mathcal{G}_2}(q)$. Utilizing the global SA-RoD rigidity of $(\mathcal{G}_1(A_1, D_1), p)$ and $(\mathcal{G}_2(A_2, D_2), q)$, there exist $c_i > 0, \theta_i \in [0, 2\pi), \xi_i \in \mathbb{R}^2$ for $i = 1, 2$ such that

$$p' = c_1 I_{n_1} \otimes \mathcal{R}(\theta_1)p + \mathbf{1}_{n_1} \otimes \xi_1, q' = c_2 I_{n_2} \otimes \mathcal{R}(\theta_1)q + \mathbf{1}_{n_2} \otimes \xi_2, \tag{59}$$

where $n_i = |\mathcal{V}_i|, i = 1, 2$. In particular, it holds that

$$p'_s = c_1\mathcal{R}(\theta_1)p_s + \xi_1, q'_t = c_2\mathcal{R}(\theta_1)q_t + \xi_2, \tag{60}$$

where $s = m, i$ and $t = j, k$. Similar to the proof in Lemma 7, we know that in the quadrilateral $\Diamond mijk$, SAs at vertices m, k, j and the RoD at vertice i can be completely determined from the rigidity function. Since m, j, k are non-collinear, the shape can be uniquely determined. This indicates that $c_1 = c_2, \theta_1 = \theta_2, \xi_1 = \xi_2$ in (60). Therefore, we have $r' = c_1 I_n \otimes \mathcal{R}(\theta_1)r + \mathbf{1}_n \otimes \xi_1$, i.e., $r \in S_r$. So the proof is finished. □

J Proof of Theorem 12

Proof. Necessarity: Suppose a configuration $y = [y_1^\top, \cdots, y_n^\top]^\top \in \mathbb{R}^{2n}$ satisfies $f_{\hat{\mathcal{G}}}(x) = f_{\hat{\mathcal{G}}}(y)$, where the subscript A, D is omitted in the expression $\hat{\mathcal{G}}(A, D)$. Based on Assumption 3 and Lemma 2, the subgraph spanned by $\mathcal{V}_a$ and related edges is complete and globally SA-RoD rigid. Denote $x_a = [x_1^\top, \cdots, x_{n_a}^\top]^\top, y_a = [y_1^\top, \cdots, y_{n_a}^\top]^\top$. Then $y_a \in S_{x_a}$. So there exist $c > 0, \theta \in [0, 2\pi), \xi \in \mathbb{R}^2$ such that $y_i = c\mathcal{R}(\theta)x_i + \xi$ for $i = 1, 2, \cdots, n_a$. This implies $cI_n \otimes \mathcal{R}(\theta)q + \mathbf{1}_n \otimes \xi$ is a solution to problem (15). By the localizability, the solution must be unique, i.e., $y = cI_n \otimes \mathcal{R}(\theta)x + \mathbf{1}_n \otimes \xi$. So $(\hat{\mathcal{G}}(A, D), x)$ is globally SA-RoD rigid.
Sufficiency: Suppose $y = [y_1^\top, \cdots, y_n^\top]^\top \in \mathbb{R}^{2n}$ is a solution to (15). Then $y \in f_{\hat{\mathcal{G}}}^{-1}(f_{\hat{\mathcal{G}}}(x))$. Due to the global SA-RoD rigidity of $(\hat{\mathcal{G}}(A, D), x)$, $f_{\hat{\mathcal{G}}}^{-1}(f_{\hat{\mathcal{G}}}(x)) = S_x$. Therefore, there exist $c > 0, \theta \in [0, 2\pi), \xi \in \mathbb{R}^2$ such that $y_i = c\mathcal{R}(\theta)x_i + \xi$ for $i = 1, 2, \cdots, n$. In particular, it holds that $y_i - y_j = c\mathcal{R}(\theta)(x_i - x_j), i \in \mathcal{V}_a$. From Assumption 3, we have $n_a \geq 2$. Since $x_i = y_i$ for $i \in \mathcal{V}_a$, we have $c = \frac{||y_i - y_j||}{||x_i - x_j||} = 1,\ \theta = 0,\ \xi = 0$. Thus, $y = x$ and $(\hat{\mathcal{G}}(A, D), x, \mathcal{V}_a)$ is SA-RoD localizable. □

K Proof of Theorem 13

To facilitate the recovery of locations from bearings and distances, we define a path matrix with respect to a base vertex.

Definition K.1. Given a graph $\mathcal{G} = (\mathcal{V}, \mathcal{E})$ and any base vertex $l \in \mathcal{V}$. After fixing a spanning tree $Tr_{\mathcal{G}}$, for any vertex $i \neq l$, there exists a path $j_1, j_2, \cdots, j_i$ connecting vertex i with l. A path matrix

$P_l \in \mathbb{R}^{n\times m}$ with base vertex l is defined as

$$P_{l,ij} \triangleq \begin{cases} 1 & e_j \text{ is consistent with the orientation,} \\ -1 & e_j \text{ is opposite to the orientation,} \\ 0 & e_j \text{ is not in the chosen path.} \end{cases} \tag{61}$$

Here it is noteworthy that the definition of P_l depends on the choice of the spanning tree and elements in the l-th row are always zero. However, we can show the following relations on different choices of path matrices.

Lemma 17. *Given a graph $\mathcal{G}$, for any two path matrices P_l, P_l' with the same base vertex $l \in \mathcal{V}$, there exists a matrix $\Phi_l \in \mathbb{R}^{n\times(m-n+1)}$ such that*

$$P_l - P_l' = \Phi_l C, \tag{62}$$

where C is the graph cycle basis matrix of $\mathcal{G}$.

Proof. For any two path matrices P_l, P_l', every nonzero row of $P_l - P_l'$ represents a cycle. Utilizing the cycle basis matrix C, every row in matrix $P_l - P_l'$ can be obtained by a linear combination of rows in C. Thus, $P_l - P_l'$ can be derived by multiplying C with a suitably sized matrix Φ_l. □

Lemma 18. *Given a framework $(\mathcal{G}, x)$, suppose that P_l is a path matrix with base vertex l, $B = [\cdots, b_{ij}, \cdots] \in \mathbb{R}^{2\times m}$ is the bearing matrix, and $d = [\cdots, d_{ij}, \cdots]^\top \in \mathbb{R}^m$ is the distance vector of all edges, then it holds that*

$$x = \mathbf{1}_n \otimes x_l + P_l \odot Bd.$$

Proof. Denote $y = \mathbf{1}_n \otimes x_l + P_l \odot Bd$. First, we will show that y is well defined, i.e., different choices of path matrices P_l, P_l' will not affect the definition of y. Let $y' = \mathbf{1}_n \otimes x_l + P_l' \odot Bd$. From equation (62), there exists a matrix $\Phi_l \in \mathbb{R}^{n\times(m-n+1)}$ such that

$$y - y' = (P_l - P_l') \odot Bd = [\Phi_l C] \odot Bd = \Phi_l C_b d = 0. \tag{63}$$

Then, we can calculate each component of y to conclude that $y = x$. □

Proof of Theorem 13. Denote the solution set of (15) and (18) as $\mathcal{S}_1$ and $\mathcal{S}_2$, respectively. We construct a map $T: \mathcal{S}_1 \to \mathcal{S}_2$ as

$$T(x) = [\cdots, ||x_j - x_i||, \frac{x_j^\top - x_i^\top}{||x_j - x_i||}, \cdots]^\top, \ (i,j) \in \hat{\mathcal{E}}.$$

It is direct to show that T is well defined. In the following, we will verify its bijectivity.
Step 1: we will prove that T is injective. Suppose $T(x) = T(y)$ for $x, y \in \mathcal{S}_1$. By the definition, $||x_j - x_i|| = ||y_j - y_i||$, $\frac{x_j - x_i}{||x_j - x_i||} = \frac{y_j - y_i}{||y_j - y_i||}$ for $(i,j) \in \mathcal{E}$. So $x_j - x_i = y_j - y_i$ for $(i,j) \in \mathcal{E}$. It means that the relative displacements of any corresponding edges in two frameworks are equal. By

the connectivity of graph $\mathcal{G}$, $x_j - x_1 = y_j - y_1$ for any $j \in \mathcal{V}$. Since sensor 1 is an anchor, $x_1 = y_1$. It can be concluded that $x = y$.

Step 2: To show T is surjective, suppose $[\cdots, d_{ij},\ b_{ij}^\top, \cdots]^\top \in \mathcal{S}_2$, we need to find a $x \in \mathcal{S}_1$ such that $T(x) = [\cdots, d_{ij},\ b_{ij}^\top, \cdots]^\top$. First, without loss of generality, let $x_1 = p_1$. Based on Lemma 18, $x = \mathbf{1}_n \otimes x_1 + P_1 \odot Bd$. If $(i,j) \in \mathcal{E}$, without loss of generality, assume that the shortest path $t_1, t_2, \cdots, t_i$ connecting vertex i with base vertex 1 does not pass vertex j, otherwise we can exchange the order of i, j. And the path consisting of $t_1, t_2, \cdots, t_i$ and edge (i,j) ends with vertex j. By previous arguments, we can modify path matrix P_1 by changing the i-th and j-th rows using these constructed paths without affecting x. Thus, the i-th and j-th rows only differ in the edge $(i,j) \in \mathcal{E}$. Thus, it follows that $x_j - x_i = d_{ij} b_{ij}$. Since $d_{ij} > 0$ and $||b_{ij}|| = 1$ hold for $(i,j) \in \hat{\mathcal{E}}$, we obtain that $||x_i - x_j|| = d_{ij}$, $\frac{x_i - x_j}{||x_i - x_j||} = b_{ij}$. On the other hand, the first two equations in constraints of (18) can transformed into those of (15). So the proof is finished. □

L Proof of Proposition 3

Proof. We will prove the statement by induction on n. In particular, C_B can be chosen as a square matrix. If $n = 3$, the framework is a triangle with anchors $1 \in \mathcal{V}_D, 2 \in \mathcal{V}_A$ and the free node $3 \in \mathcal{V}_D$. One can verify that $\text{rank}(C_B) = 6$. Then we suppose that for a framework $(\hat{\mathcal{G}}(A, D), x)$ constructed by a Type (D_1, A_1) bilateration ordering, $\text{rank}(C_{B,n}) = 4n - 6$. Here a subscript n is added in the expression $C_{B,n}$ to indicate the number of vertices. The goal is to show after adding the $n+1$-th vertice, $\text{rank}(C_{B,n+1}) = \text{rank}(C_{B,n}) + 4 = 4n - 2$. According to the parity nature of $n+1$, we discuss as follows:

Case 1: If $n+1$ is even, node $n+1 \in \mathcal{V}_A$. Assume two edges $(n+1, i), (n+1, j) \in \mathcal{E}$ are added satisfying $i, j \in \mathcal{V}_D, i < j < n+1$. One can find a path connecting nodes i and j in original graph. Note that the path $(i, n+1, j)$ also connects nodes i and j. These two paths are distinct due to the existence of node $n+1$. Thus, a new cycle can be obtained. This corresponds to adding a sub-matrix $[*, \pm d_{2n-2} I_2, \pm d_{2n-1} I_2] \in \mathbb{R}^{2 \times (4n-2)}$. On the other hand, the SA $\theta_{n+1,i,j}$ between edges $(n+1, i), (n+1, j)$ corresponds to a sub-matrix $[\mathbf{0}, \mathcal{R}(\theta_{n+1,i,j}), -I_2] \in \mathbb{R}^{2 \times (4n-2)}$. So the matrix $C_{B,n+1} \in \mathbb{R}^{(4n-2) \times (4n-2)}$ has the following blocked structure:

$$C_{B,n+1} = \begin{bmatrix} C_{B,n} & \mathbf{0} & \mathbf{0} \\ * & d_{2n-2} I_2 & \pm d_{2n-1} I_2 \\ \mathbf{0} & \mathcal{R}(\theta_{n+1,i,j}) & -I_2 \end{bmatrix}.$$

Since $\text{rank}(C_{B,n}) = 4n-6$, $C_{B,n} \in \mathbb{R}^{(4n-6)\times(4n-6)}$ is nonsingular. The non-zero subblock $C_{B,n+1}(4n-5 : 4n-4, 1 : 4n-6)$ can be tranformed to $\mathbf{0}$ by Gaussian elimination method without affecting other subblocks. So it follows that

$$\text{rank}(C_{B,n+1}) = \text{rank}(C_{B,n}) + \text{rank} \begin{bmatrix} \pm d_{2n-2} I_2 & \pm d_{2n-1} I_2 \\ \mathcal{R}(\theta_{n+1,i,j}) & -I_2 \end{bmatrix}.$$

If $\theta_{n+1,i,j} \neq 0 \mod \pi$, the rank for the last term on the RHS is 4. Otherwise, points $n+1, i, j$ are collinear. We consider the case that point $n+1$ lies on the segment connecting point i and point j (other cases can be handled similarly, here we omit the details). Then, the 4-by-4 sub-matrix at the bottom-right block of the matrix $C_{B,n+1}$ is $\begin{bmatrix} d_{2n-2}I_2 & d_{2n-1}I_2 \\ I_2 & -I_2 \end{bmatrix}$, whose rank is 4. We can conclude that $\text{rank}(C_{B,n+1}) = \text{rank}(C_{B,n}) + 4 = 4n - 2$.

Case 2: If $n+1$ is odd, we have $n+1 \in \mathcal{V}_D$. Without loss of generality, assume that two edges $(n+1, i), (n+1, j) \in \mathcal{E}$ are added satisfying $i \in \mathcal{V}_A, j \in \mathcal{V}_D, i < j < n+1$. Similarly, the newly generated cycle corresponds to a sub-matrix $[*, \pm l_{2n-2}I_2, \pm l_{2n-1}I_2] \in \mathbb{R}^{2\times(4n-2)}$. On the other hand, the SA $\theta_{i,i_0,n+1}$ between edge $(i, n+1)$ and edge (i, i_0) corresponds to a sub-matrix $[\mathbf{0}, \mathcal{R}(\theta_{i,i_0 n+1}), \mathbf{0}, -I_2, \mathbf{0}] \in \mathbb{R}^{2\times(4n-2)}$. For convenience, we represent this submatrix as $[*, -I_2, \mathbf{0}]$. So the matrix $C_{B,n+1} \in \mathbb{R}^{(4n-2)\times(4n-2)}$ can be written as:

$$C_{B,n+1} = \begin{bmatrix} C_{B,n} & \mathbf{0} & \mathbf{0} \\ * & \pm l_{2n-2}I_2 & \pm l_{2n-1}I_2 \\ * & -I_2 & \mathbf{0} \end{bmatrix}.$$

Similarly, $\text{rank}(C_{B,n+1}) = 4n - 2$. Thus, we finished the proof. $\square$

M Proof of Lemma 9

Proof. The affine structure of the solution spaces for linear equations is a standard result in linear algebra. To consider dimensions of the solution spaces, we take V_A for example. Denote $\tilde{V}_A$ as the solution space of the following homogeneous equation

$$\begin{cases} b_{ik} - \mathcal{R}(\theta_{ijk})b_{ij} = 0, \ (i,j,k) \in \mathcal{T}_{\hat{A}}, \\ \qquad\qquad b_{ij} = 0, \ i,j \in \mathcal{V}_a. \end{cases}$$

Then, $\tilde{V}_A$ is a linear space, and V_A can be viewed as a translation of $\tilde{V}_A$. Moreover, $\dim(\tilde{V}_A) = \dim(V_A)$. Since $\mathcal{T}_{\hat{A}}$ has c_A connected components, the edge set can be divided into c_A subsets, i.e., $\mathcal{E} = \cup_{i=1}^{c_A}\mathcal{E}_i$. Denote

$$W_i = \{x = [x_1, x_2, \cdots, x_{2m}]^\top \in \mathbb{R}^{2m} : x_{2t-1} = x_{2t} = 0 \text{ for } t \notin \mathcal{E}_i\}, i = 1, 2, \cdots, c_A.$$

Then, there exists a direct sum decomposition $\mathbb{R}^{2m} = \oplus_{i=1}^{C_A} W_i$. It follows that $\tilde{V}_A = \oplus_{i=1}^{C_A}(\tilde{V}_A \cap W_i)$, which means that we only need to solve (64) on each component. without loss of generality, assume the edges among anchors belong to $\mathcal{E}_1$. Based on the connectivity of the component $\mathcal{E}_1$, $\tilde{V}_A \cap W_1 = 0$. For each component $\mathcal{E}_i (i \neq 1)$, choose one edge $(u, v) \in \mathcal{E}_i$. There exists a rotation angle $\theta_{uv,st}$ such that $b_{st} = \mathcal{R}(\theta_{uv,st})b_{uv}$ for every edge $(s,t) \in \mathcal{E}_i$. In addition, we have

$$\begin{aligned} \tilde{V}_A \cap W_i = \{x \in \mathbb{R}^{2m} : & [x_{2t-1}, x_{2t}]^\top = \mathcal{R}(\theta_{i_0,t})[x_{2i_0-1}, x_{2i_0}]^\top \text{ for } t \in \mathcal{E}_i; \\ & x_{2t-1} = x_{2t} = 0 \text{ for } t \notin \mathcal{E}_i\}, \end{aligned}$$

$$
\begin{aligned}
&= \mathrm{span}\{[\mathbf{0}, 1, 0, [1,0]\mathcal{R}^\top(\theta_{i_0 i_1}), \cdots, [1,0]\mathcal{R}^\top(\theta_{i_0 i_{m_i}}), \mathbf{0}]^\top, \\
&\quad [\mathbf{0}, 0, 1, [0,1]\mathcal{R}^\top(\theta_{i_0 i_1}), \cdots, [0,1]\mathcal{R}^\top(\theta_{i_0 i_{m_i}}), \mathbf{0}]^\top\},
\end{aligned} \tag{64}
$$

where $\theta_{i_0 i_j}$ is SA between from the direction of edge i_0 to that of i_j and can be uniquely determined from (64). Consequently, $\dim(\tilde{V}_A \cap W_i) = 2$ for $i \neq 1$. Therefore, $\dim(\tilde{V}_A) = \sum_{i=1}^{c_A} \dim(\tilde{V}_A \cap W_i) = 2c_A - 2$. □

References

[1] Olfati-Saber, R. & Murray, R. M. Consensus problems in networks of agents with switching topology and time-delays. *IEEE Trans. Automat. Control* **49**, 1520–1533 (2004).

[2] Wang, L. & Xiao, F. A new approach to consensus problems in discrete-time multiagent systems with time-delays. *Sci. China Inf. Sci.* **50**, 625–635 (2007).

[3] Wang, L. & Xiao, F. Finite-time consensus problems for networks of dynamic agents. *IEEE Trans. Automat. Control* **55**, 950–955 (2010).

[4] Xiao, F. & Wang, L. Consensus protocols for discrete-time multi-agent systems with time-varying delays. *Automatica* **44**, 2577–2582 (2008).

[5] Jing, G. & Wang, L. Multiagent flocking with angle-based formation shape control. *IEEE Trans. Automat. Control* **65**, 817–823 (2020).

[6] Olfati-Saber, R. Flocking for multi-agent dynamic systems: algorithms and theory. *IEEE Trans. Automat. Control* **51**, 401–420 (2006).

[7] Wang, L., Shi, H., Chu, T., Zhang, W. & Zhang, L. Aggregation of foraging swarms. In *Proc. Int. Conf. Intelligent Computing*, vol. 3339 of *Lecture Notes in Computer Science*, 766–777 (Springer, 2004).

[8] Jing, G., Zhang, G., Lee, H. W. & Wang, L. Weak rigidity theory and its application to formation stabilization. *SIAM J. Control Optim.* **56**, 2248–2273 (2018).

[9] Oh, K.-K., Park, M.-C. & Ahn, H.-S. A survey of multi-agent formation control. *Automatica* **53**, 424–440 (2015).

[10] Han, Z., Lin, Z. & Fu, M. A survey on distributed network localization from a graph laplacian perspective. *J. Systems Sci. Complexity* **37**, 273–293 (2024).

[11] Molzahn, D. K., Dörfler, F., Sandberg, H., Low, S. H. & Cha, S. A survey of distributed optimization and control algorithms for electric power systems. *IEEE Trans. Smart Grid* **8**, 2941–2962 (2017).

[12] Zhao, S. & Zelazo, D. Bearing rigidity and almost global bearing-only formation stabilization. *IEEE Trans. Autom. Control* **61**, 1255–1268 (2016).

[13] Jing, G., Zhang, G., Lee, H. W. J. & Wang, L. Angle-based shape determination theory of planar graphs with application to formation stabilization. *Automatica* **105**, 117–129 (2019).

[14] Chen, L., Cao, M. & Li, C. Angle rigidity and its usage to stabilize multiagent formations in 2-D. *IEEE Trans. Autom. Control* **66**, 3667–3681 (2021).

[15] Huang, J. & Jing, G. Signed angle rigid graphs for network localization and formation control. *arxiv: 2505.19945* (2025).

[16] Cao, K., Han, Z., Li, X. & Xie, L. Ratio-of-distance rigidity theory with application to similar formation control. *IEEE Trans. Autom. Control* **65**, 2598–2611 (2020).

[17] Barooah, P. & Hespanha, J. P. Estimation from relative measurements: Electrical analogy and large graphs. *IEEE Trans. Signal Process.* **56**, 2181–2193 (2008).

[18] Lin, Z., Fu, M. & Diao, Y. Distributed self localization for relative position sensing networks in 2D space. *IEEE Trans. Signal Process.* **63**, 3751–3761 (2015).

[19] Biswas, P. & Ye, Y. Semidefinite programming for ad hoc wireless sensor network localization. In *Proc. 3rd Int. Symp. Inf. Process. Sensor Netw.*, 46–54 (2004).

[20] Cros, C., Amblard, P. O., Prieur, C. & Rocha, J. F. D. Pseudorange rigidity and solvability of cooperative GNSS positioning. *IEEE Trans. Control Netw. Syst.* **12**, 1176–1187 (2025).

[21] Zhao, S. & Zelazo, D. Localizability and distributed protocols for bearing-based network localization in arbitrary dimensions. *Automatica* **69**, 334–341 (2016).

[22] Li, X., Luo, X. & Zhao, S. Globally convergent distributed network localization using locally measured bearings. *IEEE Trans. Control Netw. Syst.* **7**, 245–253 (2020).

[23] Jing, G., Wan, C. & Dai, R. Angle-based sensor network localization. *IEEE Trans. Autom. Control* **67**, 840–855 (2022).

[24] Chen, L., Cao, K., Xie, L., Li, X. & Feroskhan, M. 3-D network localization using angle measurements and reduced communication. *IEEE Trans. Signal Process.* **70**, 2402–2415 (2022).

[25] Eren, T. Using angle of arrival (bearing) information for localization in robot networks. *Turk. J. Electr. Eng. Comput. Sci.* **15**, 169–186 (2007).

[26] Cao, K., Li, D. & Xie, L. Bearing-ratio-of-distance rigidity theory with application to directly similar formation control. *Automatica* **109**, 108540 (2019).

[27] Kwon, S. H., Sun, Z., Anderson, B. D. O. & Ahn, H. S. Hybrid rigidity theory with signed constraints and its application to formation shape control in 2-d space. In *Proc. 59th IEEE Conf. Decis. Control(CDC)*, 518–523 (Jeju, South Korea, 2020).

[28] Fang, X., Li, X. & Xie, L. 3-D distributed localization with mixed local relative measurements. *IEEE Trans. Signal Process.* **68**, 5869–5881 (2020).

[29] Fang, X., Li, X. & Xie, L. Angle-displacement rigidity theory with application to distributed network localization. *IEEE Trans. Autom. Control* **66**, 2574–2587 (2021).

[30] Stacey, G. & Mahony, R. The role of symmetry in rigidity analysis: A tool for network localization and formation control. *IEEE Trans. Autom. Control* **63**, 1313–1328 (2018).

[31] Eren, T. *et al.* Rigidity, computation, and randomization in network localization. In *Proc. IEEE INFOCOM*, vol. 4, 2673–2684 (2004).

[32] Eren, T. Cooperative localization in wireless ad hoc and sensor networks using hybrid distance and bearing (angle of arrival) measurements. *J. Wireless Com. Netw.* **72**, 1–18 (2011).

[33] Lin, Z., Han, T., Zheng, R. & Yu, C. Distributed localization with mixed measurements under switching topologies. *Automatica* **76**, 251–257 (2017).

[34] Girolami, M., Barsocchi, P., Furfari, F., Rosa, D. L. & Mavilia, F. Evaluation of angle of arrival in indoor environments with bluetooth 5.1 direction finding. In *2022 18th International Conference on Wireless and Mobile Computing, Networking and Communications (WiMob)*, 284–289 (IEEE, 2022).

[35] Trinh, M. H., Tran, Q. V. & Ahn, H.-S. Minimal and redundant bearing rigidity: Conditions and applications. *IEEE Trans. Autom. Control* **65**, 4186–4200 (2019).

[36] Asimow, L. & Roth, B. The rigidity of graphs. *Trans. Amer. Math. Soc.* **245**, 279–289 (1978).

[37] Jackson, B. & Jordán, T. Connected rigidity matroids and unique realizations of graphs. *J. Combin. Theory Ser. B* **94**, 1–29 (2005).

[38] Connelly, R. Generic global rigidity. *Discrete Comput. Geom.* **33**, 549–563 (2005).

[39] Wan, C., Jing, G., You, S. & Dai, R. Sensor network localization via alternating rank minimization algorithms. *IEEE Trans. Control Netw. Syst.* **7**, 1040–1051 (2019).

[40] Eren, T., Anderson, B. D. O., Whiteley, W., Morse, A. & Belhumeur, P. Merging globally rigid formations of mobile autonomous agents. In *Proc. of the 3rd IEEE international joint conference on autonomous agents and multiagent systems*, 1260–1261 (2004).

[41] Arrigoni, F. & Fusiello, A. Bearing-based network localizability: A unifying view. *IEEE Trans. Pattern Anal. Mach. Intell.* **41**, 2049–2069 (2019).

[42] Ruszczyński, A. *Nonlinear Optimization* (Princeton University Press, 2011).

[43] Godsil, C. & Royle, G. F. *Algebraic Graph Theory*, vol. 207 of *Grad. Texts in Math.* (Springer, New York, 2001).

[44] Connelly, R. & Guest, S. D. *Frameworks, Tensegrities, and Symmetry* (Cambridge University Press, 2022).

[45] Zhao, S., Sun, Z., Zelazo, D., Trinh, M.-H. & Ahn, H.-S. Laman graphs are generically bearing rigid in arbitrary dimensions. In *Proc. 56th IEEE Conf. Decis. Control (CDC)*, 3356–3361 (Melbourne, VIC, Australia, 2017).

[46] Lee, J. *Introduction to Smooth Manifolds*, vol. 218 of *Grad. Texts in Math.* (Springer, New York, 2000).

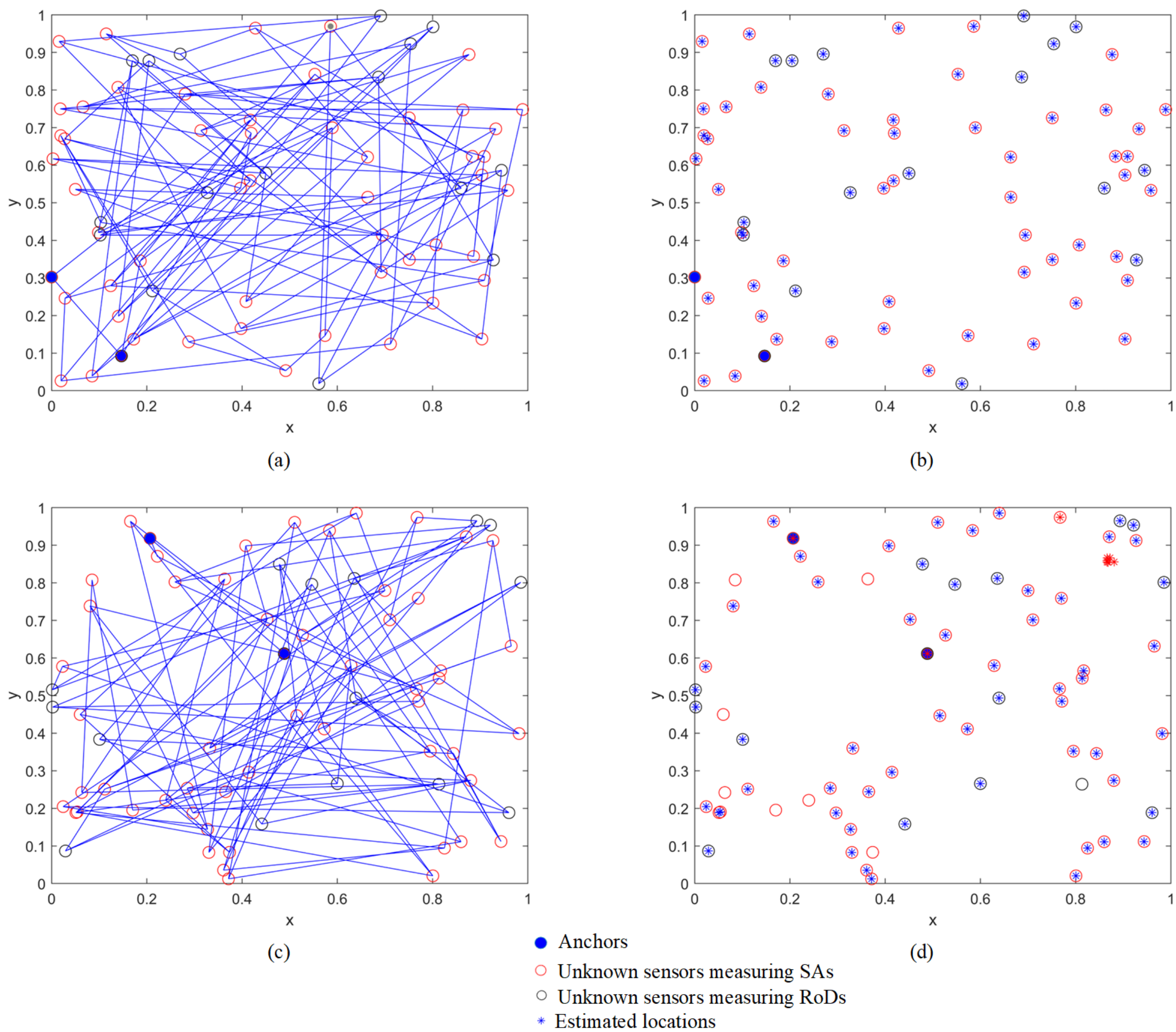

Fig. 11. (a) A quadrilateralized network that is SA connected and constructed by 2-vertex additions and satisfies $\text{rank}(C_D) = 103$. (b) Estimated locations match the real locations well. (c) A quadrilateralized network that is SA connected and satisfies $\text{rank}(C_D) = 101$. (d) Some nodes (marked with red asterisks) are incorrectly localized since the whole network is unlocalizable.

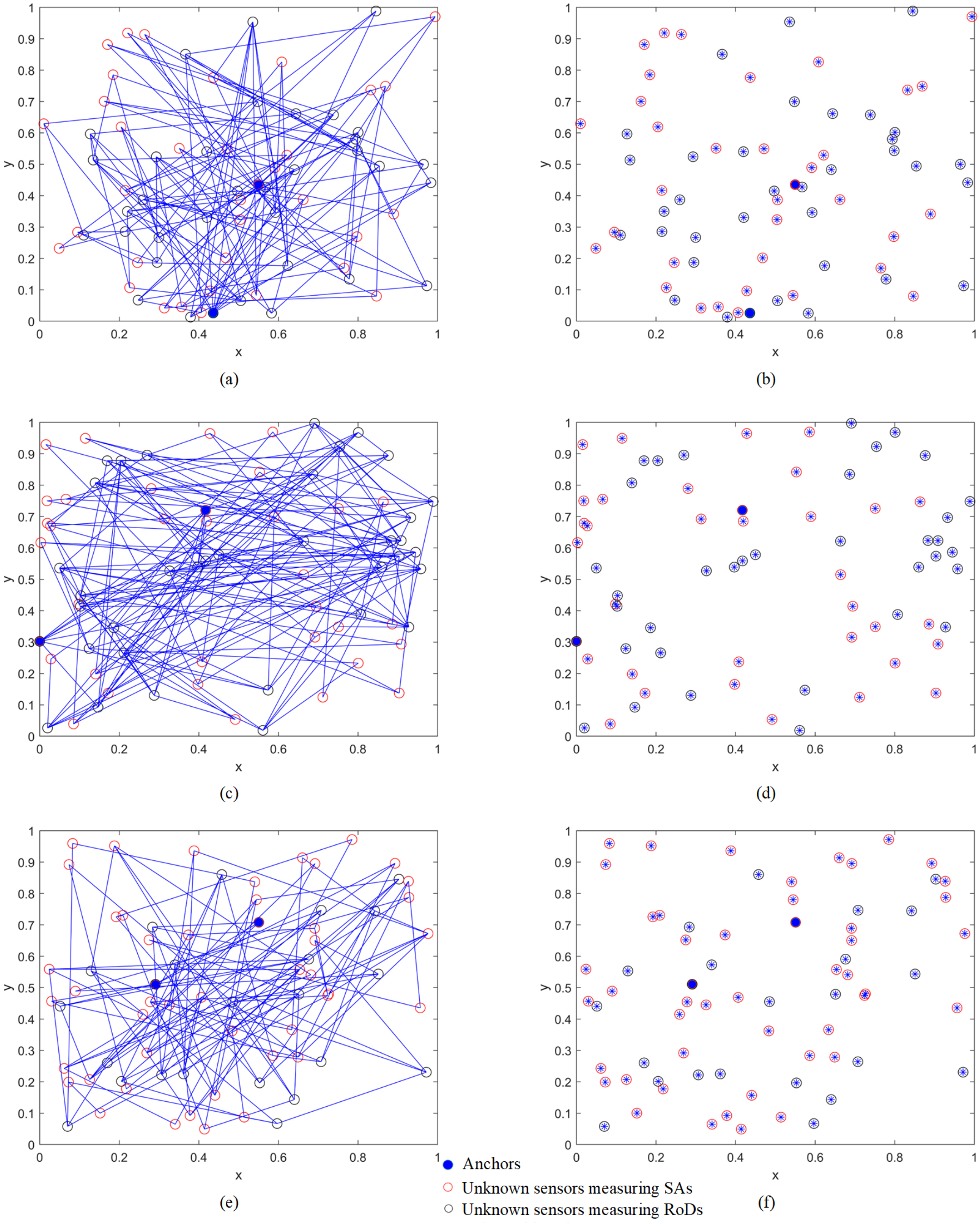

Fig. 12. (a) A RoD connected sensor network constructed by a Type (D_1, A_1) bilateration ordering. (b) Localization results. (c) A RoD connected sensor network constructed iteratively from a quadrilateral through a sequence of Type D_2 and Type A_1 1-vertex additions. (d) Localization results. (e) A sensor network constructed by a Type $(2, D_1)$ SA-RoD ordering. The SA and RoD constraints are disconnected. (f) Localization results.